8-2021

Venturi Meter Performance When Installed on the Branch of a Tee Junction with Converging Run Flow

E. Elliot Naulu
Utah State University

VENTURI METER PERFORMANCE WHEN INSTALLED ON THE BRANCH OF A TEE JUNCTION WITH CONVERGING RUN FLOW

by

E. Elliot Naulu

A thesis submitted in partial fulfillment
of the requirements for the degree

of

MASTER OF SCIENCE

in

Civil and Environmental Engineering

Approved:

_____	_____
Michael C. Johnson, Ph.D., P.E. Major Professor	Zachary B. Sharp, Ph.D., P.E. Committee Member
_____	_____
Marv Halling, Ph.D., P.E. Committee Member	D. Richard Cutler, Ph.D. Interim Vice Provost of Graduate Studies

UTAH STATE UNIVERSITY
Logan, Utah

2021

ABSTRACT

Venturi meter performance when installed on the branch of a

tee junction with converging run flow

by

E. Elliot Naulu, Master of Science

Utah State University, 2021

Major Professor: Dr. Michael C. Johnson
Department: Civil and Environmental Engineering

Venturi flow meters are often installed downstream of disturbances such as a tee junction, valve, or elbow. In such a case, laboratory calibration may be needed to measure the Venturi meter's performance under said limitations so that accurate metering is achieved. However, in some cases, laboratory calibration may not be possible. The purpose of this research was to investigate Computational Fluid Dynamics (CFD) ability to simulate a Venturi meter installed on the branch of a tee junction with converging run flow.

Physical laboratory data was collected for a 6-inch Universal Venturi Tube (UVT) flowmeter. The UVT meter was installed in a straight-line, followed by an installation on the branch of a tee junction at both zero-diameters (0D) and five-diameters (5D). CFD modelling was then used to perform the same installments for calibration and verification of the physical data. CFD was further used to simulate different tee geometries, beta ratios, and pipe sizes.

The results show that CFD is capable of modelling a Venturi meter installed in the previously mentioned configuration. While CFD performed well across all flow splits, the percent difference was smallest between physical and CFD data as the converging flow split approached a 50/50 split. Using the results, contour plots were developed that help to apply a correction factor to the given straight-line discharge coefficient to decrease uncertainty in flow measurement. This research is significant in that it provides readers with a method to adjust a Venturi meter's discharge coefficient for a Venturi that will be, or already is, installed on the branch of a tee junction with converging run flow.

(67 pages)

PUBLIC ABSTRACT

Venturi meter performance when installed on the branch

of a tee junction with converging run flow

E. Elliot Naulu

Venturi flow meters are often installed downstream of disturbances such as a tee junction, valve, or elbow. In such a case, a laboratory calibration may be needed to measure the Venturi meter's performance under said limitations so that accurate metering is achieved. However, in some cases, laboratory calibration may not be possible. The purpose of this research was to investigate Computational Fluid Dynamics (CFD) ability to simulate a Venturi meter installed on the branch of a tee junction with converging run flow.

This study used CFD to compare against laboratory results to illustrate CFD's capability as a calibration method. The results of this study were used to develop a procedure to adjust a Venturi meter's discharge coefficient for a Venturi meter that will be, or already is, installed on the branch of a tee junction with converging run flow.

ACKNOWLEDGMENTS

I would like to thank Dr. Michael Johnson for his guidance in completing this project. I would also like to thank him for the opportunity to learn under his direction at the Utah Water Research Lab.

I would also like to thank my other committee members, Dr. Zach Sharp and Dr. Marv Halling, for their support and insight. Dr. Sharp's knowledge of CFD was instrumental in helping me achieve accurate results.

Lastly, none of this would be possible without the love and support of my wife, Jamie. I'd like to thank her for her encouragement and selflessness as I've completed this research.

E. Elliot Naulu

CONTENTS

Page

LIST OF TABLES

Page

LIST OF FIGURES

Page

NOTATION

0D = Zero-diameters downstream of tee junction

5D = Five-diameters downstream of tee junction

C_d = Venturi discharge coefficient

Q = Total flow rate (lb/s)

Y = Gas expansion coefficient

D = Venturi inlet diameter (ft)

d = Venturi throat diameter (ft)

g = Acceleration due to gravity (ft/s^2)

ΔP = Differential pressure between the inlet taps and throat taps (lb/ft^2)

ρ_f = Density of water (lb/ft^3)

Q_{tank} = Total flow rate calculated from weight tank (cfs)

W = Net weight collected in the weight tank (lb)

T = Time water was being collected in weight tank (sec)

CHAPTER I

INTRODUCTION

Problem Introduction

Flow measurement is an essential parameter in many processes. For this reason, a substantial amount of research has been geared towards determining the required pipe diameters needed between pipe fittings and the Venturi meter. For example, The American Society of Mechanical Engineers (ASME) provided a range of 8 to 16 diameters for a classical Venturi meter installed downstream of a single 90-degree elbow, with the range being relative to the meter's beta ratio (ASME, 2008b). The beta ratio is defined as the ratio between the Venturi meter's throat diameter to the inlet diameter.

While a Venturi meter is most accurate when installed per the manufacture designed conditions, it is not uncommon for Venturi meter's to be installed in undesirable conditions. When this occurs, the flow profile is disturbed, and the design discharge coefficient no longer produces an accurate flow measurement. To achieve accurate flow measurement, the Venturi meter would need to be calibrated in a laboratory with the same pipe configuration as the field installation. The laboratory calibration would produce a new discharge coefficient that would properly represent the disturbed flow profile from the disturbance upstream. However, in some cases, laboratory calibration may not be possible.

One such installation is a Venturi meter placed downstream of the branch of a tee junction with converging run flow (Figure 1). This research used both

Computational Fluid Dynamics (CFD) and physical data to determine the effects this installation has on the discharge coefficients of Venturi meters. It is expected that the results of this study will provide readers with a method to adjust a Venturi meter's discharge coefficient installed in this configuration using CFD.

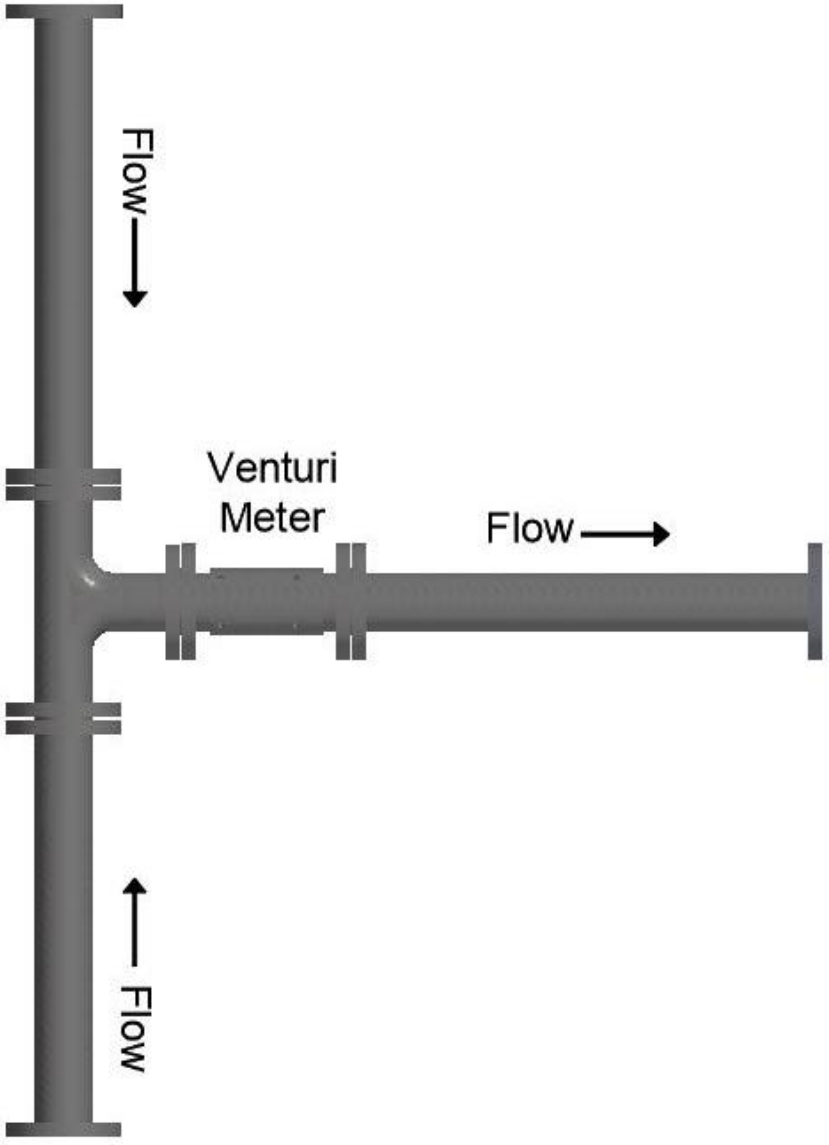

Figure 1. General configuration for research

Venturi Meter Review

The Venturi meter, named after Geovanni B. Venturi, has been used to measure flow since the 1880's (Finnemore & Franzini, 2006). The Venturi meter consists of a constricted area (throat) that causes an increase in velocity and consequently a decrease in pressure, the throat section is then followed by a diverging tube which allows for pressure recovery (Figure 2). Pressure taps located on the inlet and the throat are used to measure the differential pressure produced by the meter, which can then be applied to the Bernoulli principle and conservation of mass to calculate the flow rate using the proper flow rate equation.

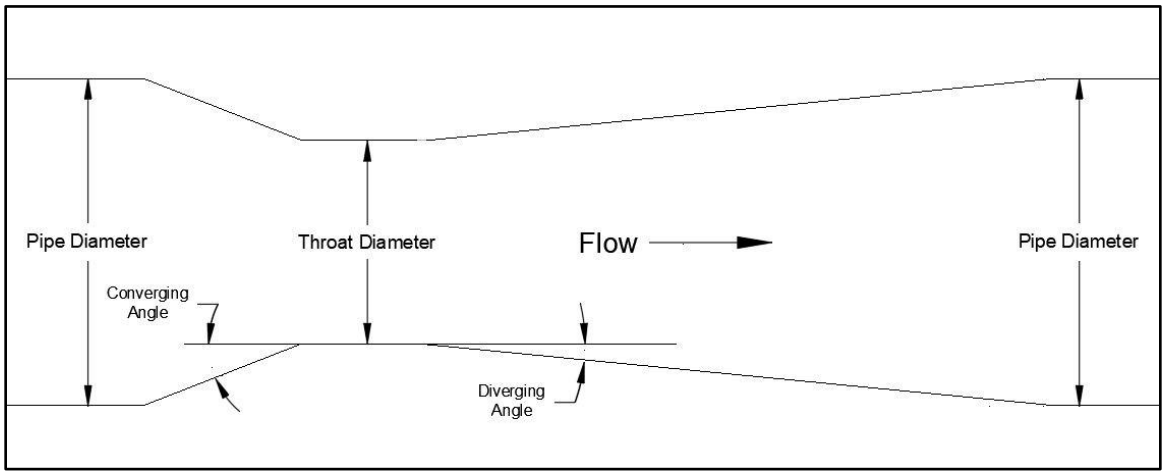

Figure 2. General geometry of a classical Venturi meter

To account for the small amount of head loss due to friction, a discharge coefficient, *C*, is assigned to each Venturi meter and is used to calculate the flow rate. The discharge coefficient is calculated using equation 1 where *Q* is the mass flow rate, *d* is the diameter of the throat, *D* is the diameter of the meter inlet, *g* is the acceleration due

to gravity, ΔP is the pressure differential, ρ_f is the density of the fluid, and Y is the gas expansion coefficient for gasses (1 for liquids).

$$C = \frac{Q}{Y\frac{\pi}{4}d^2\sqrt{\frac{2g}{1-\left(\frac{d}{D}\right)^4}} * \sqrt{\Delta P \rho_f}} \quad (1)$$

Research and manufacturing capabilities have led to several modifications to the classical Venturi meter. The most common include the Universal Venturi Tube (UVT), Halmi Venturi Tube (HVT), Dahl Tube, and the nozzle Venturi. Only the classical Venturi meter and the UVT meter were used within this study (Figure 3).

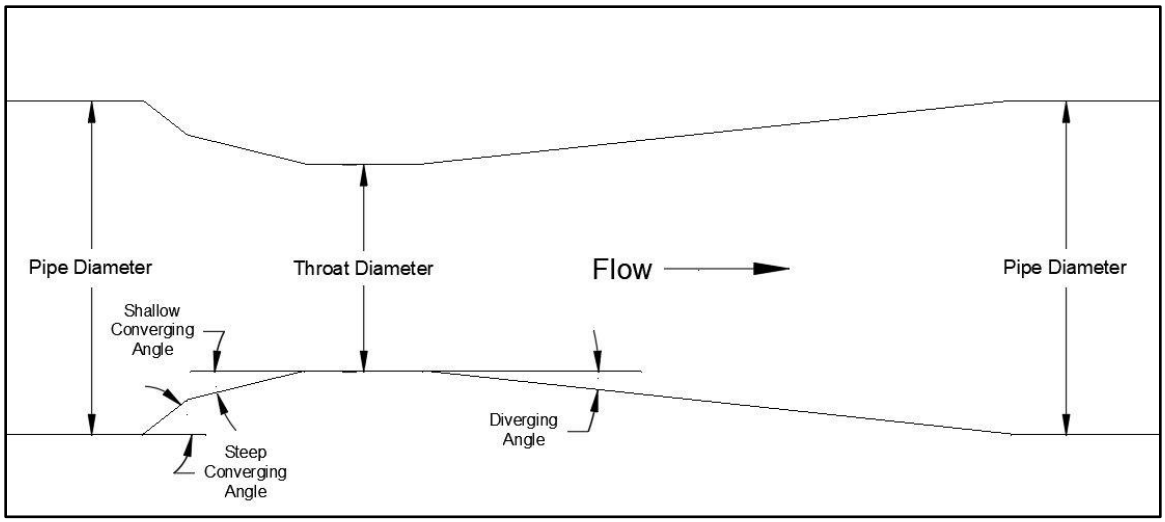

Figure 3. General geometry of a UVT meter

Computation Fluid Dynamics Review

CFD is a numerical modelling method used to analyze fluid flow and has been used in practice since the 1960's. It is a method that numerically solves the Navier-Stokes

equations and has proven quantitively its ability to predict the performance of flowmeters (Sharp, 2016). While laboratory calibrations are effective, they're not always feasible or practical. For example, if a waste water treatment plant wanted to verify the performance of their existing meter, a lab calibration may be impractical due to removing the meter from service and the cost and logistics of transporting the meter to a laboratory. While not as accurate as a laboratory calibration, CFD provides an alternative as a means to adjust a meter's discharge coefficient due to its ability to manipulate elements of a model that would otherwise be difficult to achieve within physical modelling.

Objectives

The objective of this research was to investigate CFD's ability to simulate a Venturi meter installed on the branch of a tee junction with converging run flow. The project objectives were as follows:

1) Complete a thorough literature review of research regarding flowmeter behavior when placed downstream of a disturbance.
2) Collect physical data using a 6-inch BIF Universal Venturi Tube (UVT). A straight-line test will be conducted followed by a series of tee tests. The flowmeter will be placed at both zero-diameters and five-diameters downstream of the tee junction.
3) Collect CFD data by running a straight-line simulation followed by a series of tee junction simulations imitating the physical testing described in objective 2.
4) Perform the above procedure in CFD for a 24-inch pipe configuration. Additional simulations of a 48-inch pipe will be conducted to validate the results.

5) Analyze how the tee geometry effects the performance of the described setup. The CFD simulations will include a series of sharp-cornered tee tests to compare against the round-cornered tee tests.
6) Analyze the effects the flowmeter's beta ratio has on the described setup. The CFD simulations will include a beta ratio of 0.7 along with a 0.5 beta ratio.

CHAPTER II

LITERATURE REVIEW

A thorough literature review was conducted to understand what others have presented on the topic. While no literature was found regarding the proposed research topic of converging flow in a tee junction and its effects on the accuracy of a Venturi meter, a large amount of research exists on pressure losses through tee junctions and Venturi meter performance with flow disturbances upstream.

ASME MFC-3M is a standard used to provide guidance on the proper installation of differential pressure flowmeters such as orifice plates, Venturi meters, and nozzles. While the standard does not provide a minimum distance downstream of a tee-junction for a Venturi meter installation, the standard does provide the minimum distance for a single 90° bend, which is between 8 and 16 diameters (ASME, 2008b).

Costa and colleagues compared a sharp-cornered tee to a round-cornered tee and how their geometries influence the pressure profile. They examined the flow characteristics of both the straight flow and the branched flow to develop a loss coefficient. They observed that the rounded tee generated more turbulence in the branch pipe, which resulted in a weaker and shorter recirculation bubble region and consequently a lower loss coefficient (Costa et al., 2006).

Abdulwahhab and colleagues investigated how the k-ε turbulence model predicted pressure losses in a tee junction. They analyzed the effect different area ratios of the inlets had on the pressure field and found that as the branch area decreases the velocity increases and consequently generates more recirculation and turbulence. As

expected, they concluded that higher pressure loss coefficients were a direct result of higher flow rates (Abdulwahhab et al., 2013).

Sharp researched the energy losses that occur in crosses. He developed energy loss coefficients (K-factors) for four different flow scenarios. The flow scenario that most closely resembled this research was his combining flow scenario, which had converging flow in three of the four legs with the other leg being the outlet. Sharp found that the K-factors were higher in the combining flow scenario when the leg perpendicular to the outlet leg passed majority of the flow, creating a vortex in the pipe and consequently a significant amount of energy loss (Sharp, 2009).

Stauffer researched how using a hydraulic average of multiple tap sets would improve the accuracy of a Venturi flowmeter when installed downstream of a disturbance. The disturbances upstream of the Venturi flowmeter included a short radius elbow and a butterfly valve set at both full open and 45 degrees open. Stauffer found that the uncertainty in the flow measurement decreased by half when using a hydraulic average of multiple tap sets (Stauffer, 2019).

Sandberg investigated CFD's competency in predicting flow measurement for a Venturi flowmeter installed on the branch of a tee junction with flow passing through the run. Sandberg tested different types of tees (sharp versus smooth), Venturi geometries (classical versus UVT), and distances downstream of the tee (0D, 2D, 5D, 10D). Sandberg found that the classical Venturi geometry yielded a more predictable deviation from the straight trend than the UVT geometry. Sandberg concluded that CFD effectively simulated the majority of the physical data with the exception of the low flow splits (Sandberg, 2020).

The research presented in this literature review is related to the thesis topic in that each article focuses on the improvement of flow measurement. The thesis topic is unique because it focuses on CFD's ability to simulate physical data where there is converging flow in the run of a tee junction. The research will be beneficial to flowmeter users due to the complete lack of information that exists on single-phase converging flow in a tee junction.

CHAPTER III

EXPERIMENTAL METHODS

Physical Modelling Methods

The physical laboratory data for this research was conducted at the UWRL in Logan, Utah. The model consisted of a 6-inch UVT with a beta ratio of 0.7 and a 6-inch round-cornered tee junction. A straight-line test was conducted to illustrate how the UVT meter performed under ideal conditions, and a series of zero-diameter (0D) and five-diameter (5D) runs followed. Due to the Venturi meter's performance at 5D, this study did not include testing at 10D. Appendix A shows figures of the laboratory testing and the instrumentation used to collect data to determine the discharge coefficients for the described installations.

Due to the anticipated turbulence created from the converging flow in this research, four pressure tap sets were considered (Figure 4). Each tap set consists of a high tap located on the meter's inlet and a low tap on the meter's throat. The four tap sets will help in understanding the flow profile and the impacts the tee junction and the converging flow has on the Venturi meter.

To measure the differential pressure in the laboratory, a differential pressure (DP) transmitter was used. The DP transmitter measures the change in pressure from the tap sets and sends the information as a voltage to a multimeter. The multimeter records the average voltage which is then recorded in a spreadsheet that converts the voltage to inches of H20. The same calibrated transmitters and multimeters were used for the straight-line, 0D, and 5D tests.

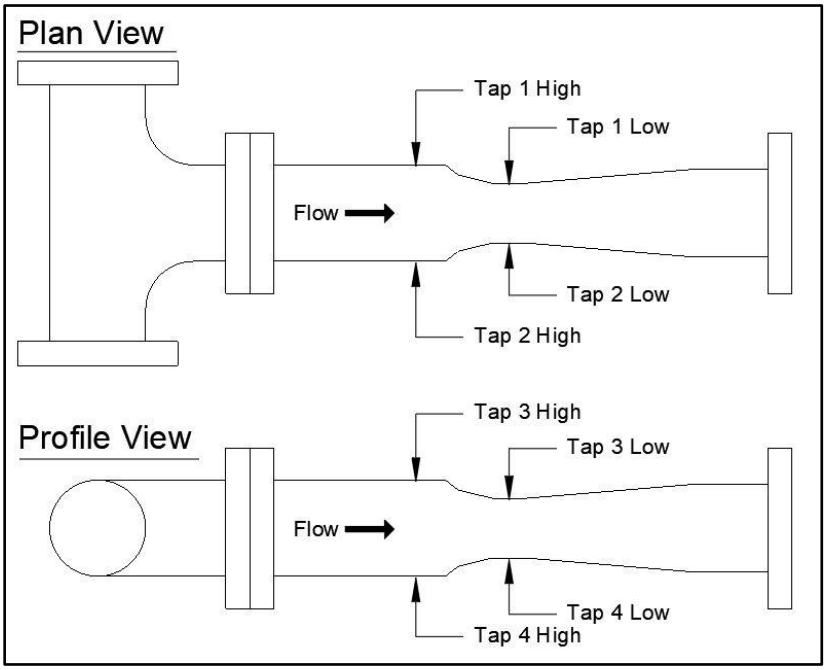

Figure 4. Tap Set Configurations

Each installation measured flow using a reference meter and a weight tank. The weight tank was used to check the accuracy of the reference meter, which is achieved by using equation 2. Where Q_{tank} is the total flow rate, W is the net weight collected in the weight tank, ρ_f is the density of water, and T is the time the water was collected for the test.

$$Q_{tank} = \frac{W}{\rho_f * T} \tag{2}$$

The UWRL has two calibrated weight tanks with weight capacities of 25,000 lb and 250,000 lb. The precision of the weight tanks is assured by the National Institute of Standards and Technology (NIST), which ensures that the calibration is metrologically

traceable to NIST standards. Both the small and large weight tanks were used for the straight-line, 0D, and 5D tests.

The straight-line test acted as a benchmark for the 0D and 5D tests. The straight-line installation had 14 feet of upstream pipe (28 diameters), which was considered sufficient to allow for a developed and uniform flow profile to form (Figure 5). The test consisted of eight data points ranging in Reynolds numbers from 71,000 to 793,000. The process to collect a single data point is as follows:

- Set the desired flow
- Start the stop watch and record the starting weight
- Start averaging the voltage output on the multimeters
- Start averaging the multimeter measuring the flow from the reference meter
- Record the temperature of the water
- Stop stopwatch at desired time (300 seconds for low flows and 200 seconds for high flows) and record the final weight
- Record the averages from multimeters

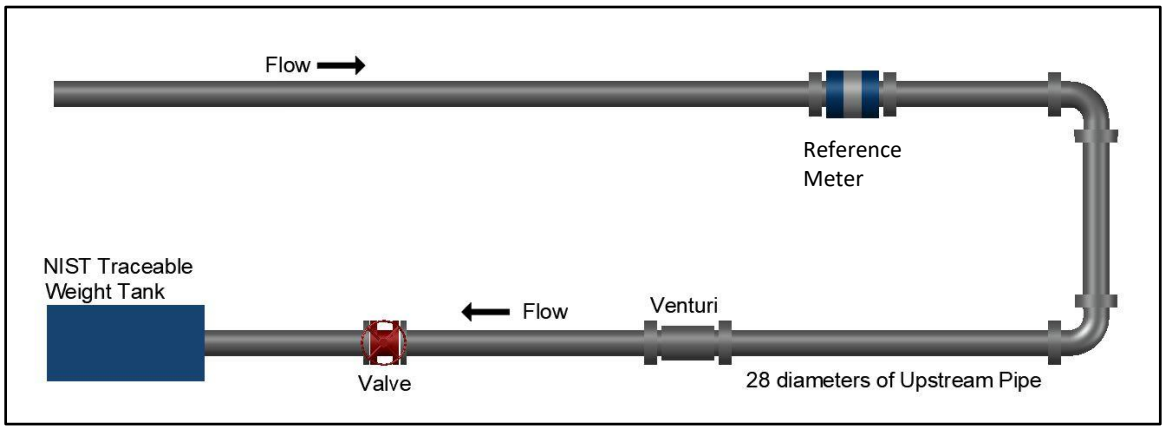

Figure 5. Straight-line Installation

Using the recorded differential pressures and flow, the C value for each tap set was calculated using equation 1. It's important to note that for the tests performed in this research the reference meter had been verified against the weight tank and accurately measured flow to ±0.31%. While the absolute accuracy was important, even more important is the consistency of the meter so that trends can be identified. The differences of the coefficient in the different installations were more important than the absolute accuracy of the flow measurement. As long as the standard is consistent, the differences will be captured.

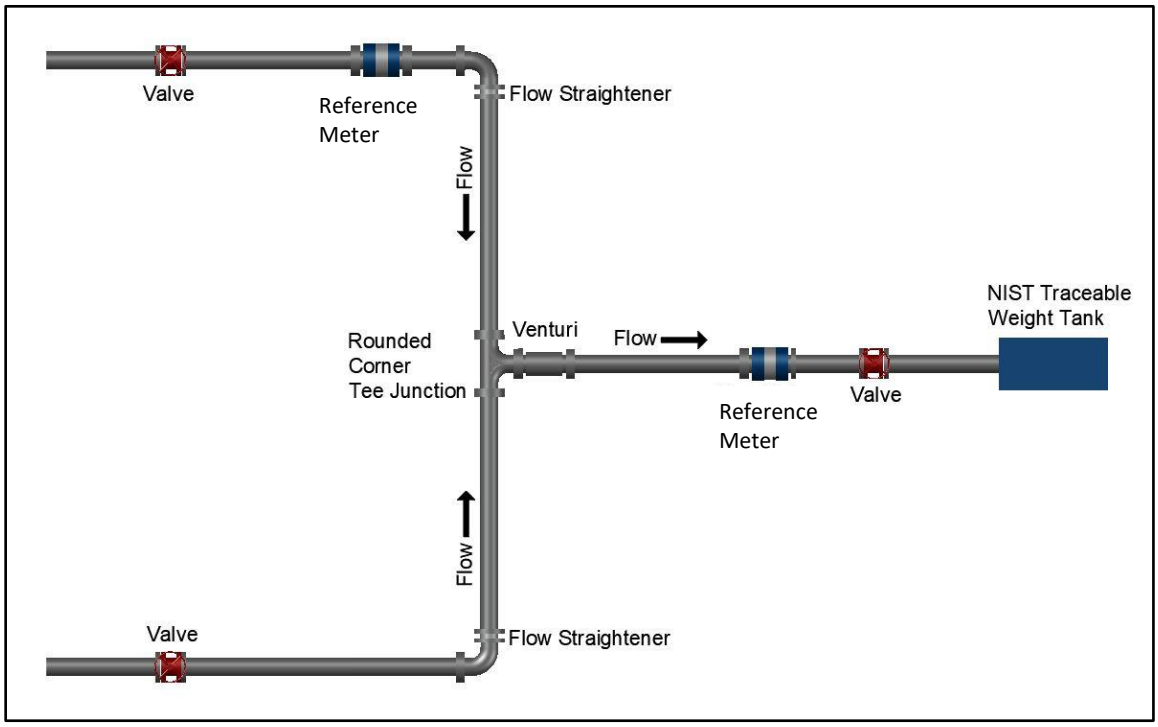

Figure 6. General Converging Flow Configuration

The 0D and 5D test setup consisted of a north line and a south line that elbowed towards each other and connected at a tee junction with the meter installed on the branch

(Figure 6). The 0D and 5D tests required two reference meters, one on the outlet to measure total flow and the other on the north line to measure one of the converging flows. The south line flow was found by simply subtracting the north line flow from the total flow. To ensure that the flow profiles entering the tee junction from the north and south lines were developed and uniform, flow straighteners were installed in each line downstream of the elbows to condition the flow and eliminate non-uniform conditions which may affect the results.

The 0D and 5D tests consisted of three flows (1800, 1200, 400 gpm), with each flow having four runs or flow splits (Table 1). The process to collect a single data point was the same as the straight-line test with the exception of having to set two flows. After collecting the data for tap sets one and two the test was repeated with the Venturi meter rotated out of plane to collect data for tap sets three and four.

Table 1. Flow splits

1800 gpm		
Run (flow split)	North Line (gpm)	South Line (gpm)
Run 1 (100/0)	1800	0
Run 2 (80/20)	1440	360
Run 3 (60/40)	1080	720
Run 4 (0/100)	0	1800
1200 gpm		
Run (flow split)	North Line (gpm)	South Line (gpm)
Run 1 (100/0)	1200	0
Run 2 (80/20)	960	240
Run 3 (60/40)	720	480
Run 4 (0/100)	0	1200
400 gpm		
Run (flow split)	North Line (gpm)	South Line (gpm)
Run 1 (100/0)	400	0
Run 2 (80/20)	320	80
Run 3 (60/40)	240	160
Run 4 (0/100)	0	400

Numerical Modelling Methods

The CFD modelling for this research was performed at the UWRL in Logan, Utah. The numerical procedure for determining the *C* values for the Venturi meter in CFD is similar to the physical tests. A straight-line numerical model was created to illustrate how the Venturi meter performed in CFD under ideal conditions, and a series of 0D and 5D simulations followed. The purpose of this method is not to replicate the absolute values of the physical models, but rather to replicate the percent change or differences from the straight-line calibration of the respective methods. It should be noted that in order to achieve accurate results and decrease simulation run times a fully developed and uniform flow profile interface was used at both the north and south inlets for the 0D and 5D simulations (Figure 7). This prevents including a long length of approach pipe upstream from the region of interest which reduces the computation time needed for a solution to converge.

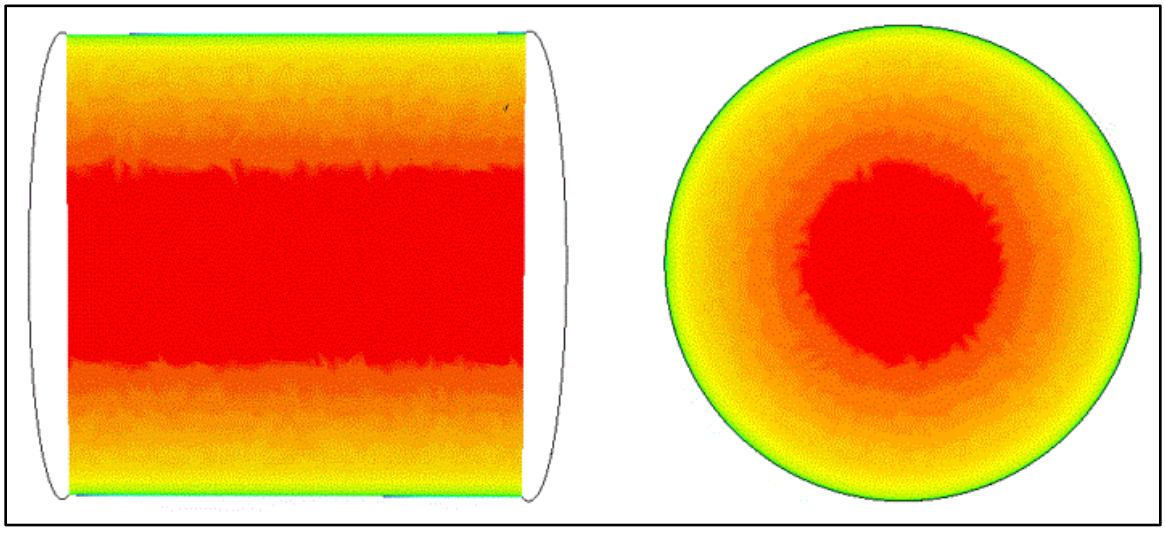

Figure 7. Fully Developed and Uniform Flow Profile Interface

CFD is capable of using different turbulence models to generate a solution. Some of these turbulence models include Reynolds-Averaged Navier Stokes (RANS), Detached Eddy, and Large Eddy. The physics models used in this research included: three-dimensional space, steady state, liquid material, segregated flow, gradients, constant density, turbulent regime, RANS model, K-Epsilon turbulence model, two-layer all y + wall treatment, realizable K-Epsilon two-layer, and exact wall distance.

Essential to any CFD model is its computational mesh or grid (Figure 8). In order to analyze fluid flow numerically, the system is divided into small cells. Each cell passes information to the next making the transition from cell to cell essential. An inaccurate mesh can lead to extensive run times or a solution that doesn't converge. While the number of prism layers, prism layer stretching, and the prism layer thickness were adjusted to achieve the most accurate results, the same base size was used for all 6-inch simulations. The meshing models used in this research included: surface remesher, polyhedral mesher, and prism layer mesher.

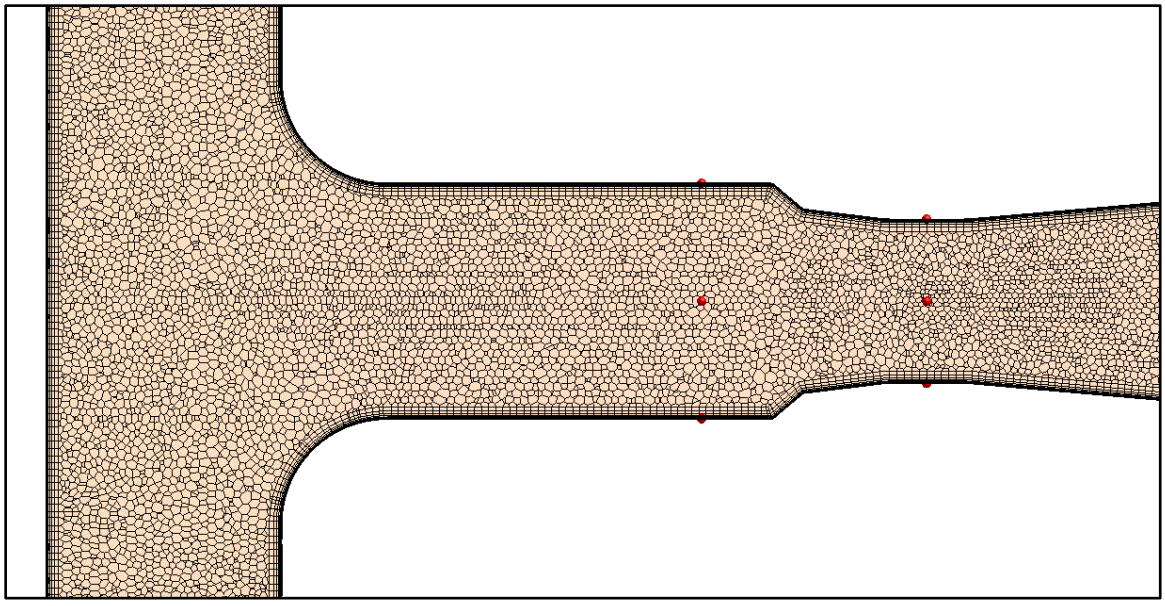

Figure 8. Mesh of the 6-inch UVT meter at 0D from the tee junction

Contour Plots

For this research, contour plots were used to help readers understand the process to adjust the discharge coefficient. Using a Python code developed by Ben Sandberg and Taylor Vaughn, the contour plots contain discharge coefficient ratios plotted against flow split and meter Reynolds number. Sandberg's code was used in his research to create contour plots of a Venturi meter installed on the exit branch of a tee with flow splitting between the run and the branch. Due to similarities between Sandberg's and this research, his code was used to maintain a consistent methodology for those interested in this research. Appendix C of Sandberg's thesis contains the specifics concerning this methodology (Sandberg, 2020).

For the 6-inch 0D and 5D contour plots found in appendix B, the Reynolds number was extended to 2 million to see if the $C/C_{straight}$ values converged to a specific flow split at higher Reynolds numbers. As anticipated, flow split three for tap sets three and four stabilized while flow splits one and two were more erratic. It should be noted that the residuals from all CFD simulations converged below $1x10^{-3}$, which is generally accepted as the minimum degree of convergence.

CHAPTER IV

RESULTS AND DISCUSSION

6-inch Verification

The Venturi meter's performance downstream of the tee junction was illustrated using plots of percent deviation from the straight-line *C* value versus the Reynolds number entering the meter. The 6-inch UVT was modelled first to validate the physical data. The CFD models included a straight-line test followed by a series of 0D and 5D tests. Additional models followed to illustrate trends in the CFD data, these included changes in tee geometry, beta ratio, and pipe size.

The comparison between the laboratory and CFD straight-line tests are shown in Figure 9. The average *C* value for tap set one and two for the laboratory data were 0.9818 and 0.9794, respectively. The CFD data yielded an average *C* value of 0.9640 for both tap sets, which equates to -1.9% shift for tap set one and a -1.7% shift for tap set two.

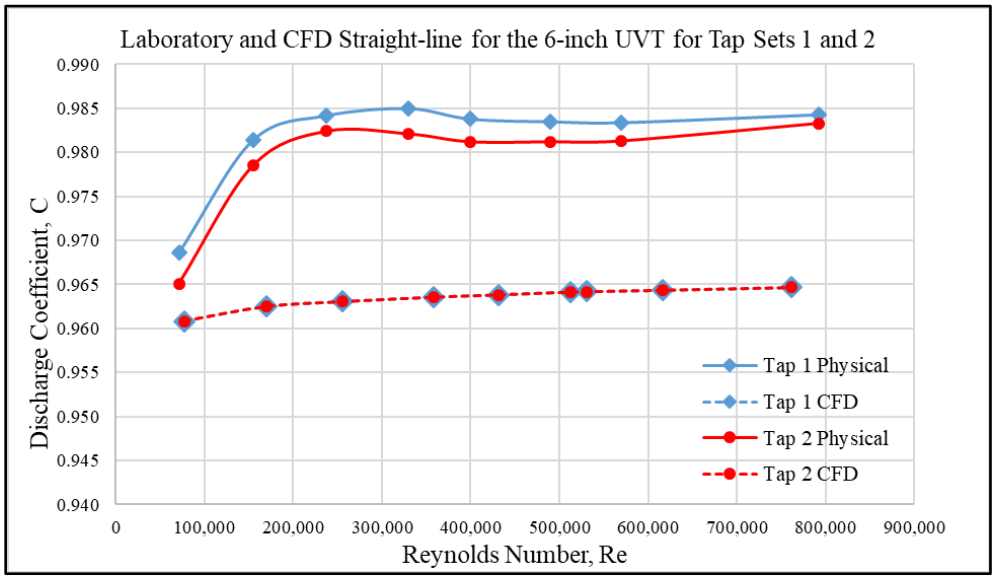

Figure 9. 6-inch UVT straight-line calibration

Figure 10 shows the laboratory results with the CFD simulations for the four tap sets at 0D, while Figure 11 shows the results for the 5D installation. The percent deviation was calculated using interpolation for the straight-line *C* values to ensure the Reynolds numbers were the same at each flow split for the 0D and 5D installations. From the figures, it quickly becomes apparent that CFD models the physical trends better in tap sets three and four than in tap sets one and two.

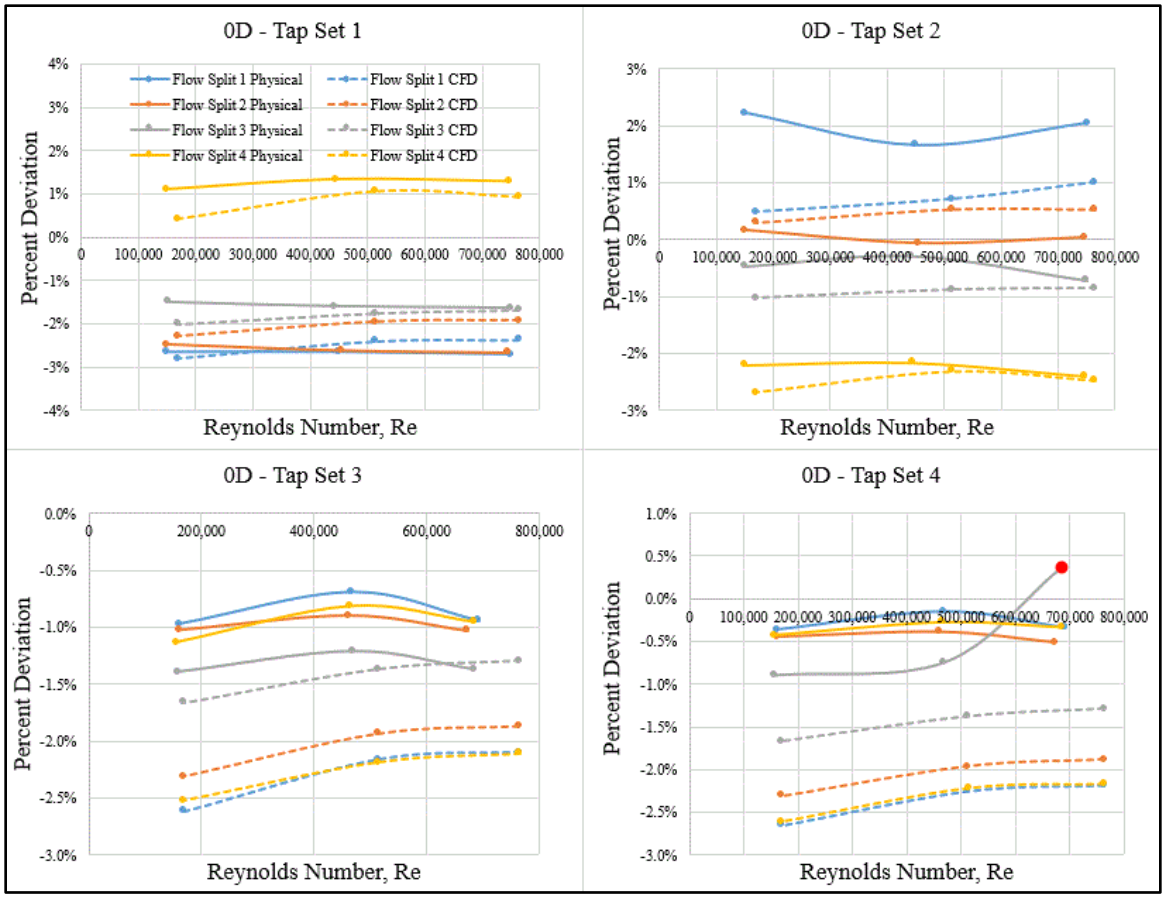

Figure 10. Physical and CFD results for all tap sets at 0D. The red dot seen in the tap set four graph illustrates an outlier in the physical data

From Figure 11, it should be stressed that the CFD results for flow split four of tap set two and flow split one of tap set one do not adequately follow the physical trend at the lower Reynolds number. This is significant because if one were to use the CFD results for these configurations to adjust the given discharge coefficient, their solution would actually be more incorrect than if they were to do nothing and simply use the given discharge coefficient. Therefore, these configurations should be avoided. It should be noted that the highest deviation at any flow split of CFD to physical was 1.7% for 0D and 1.9% for 5D for all tap sets.

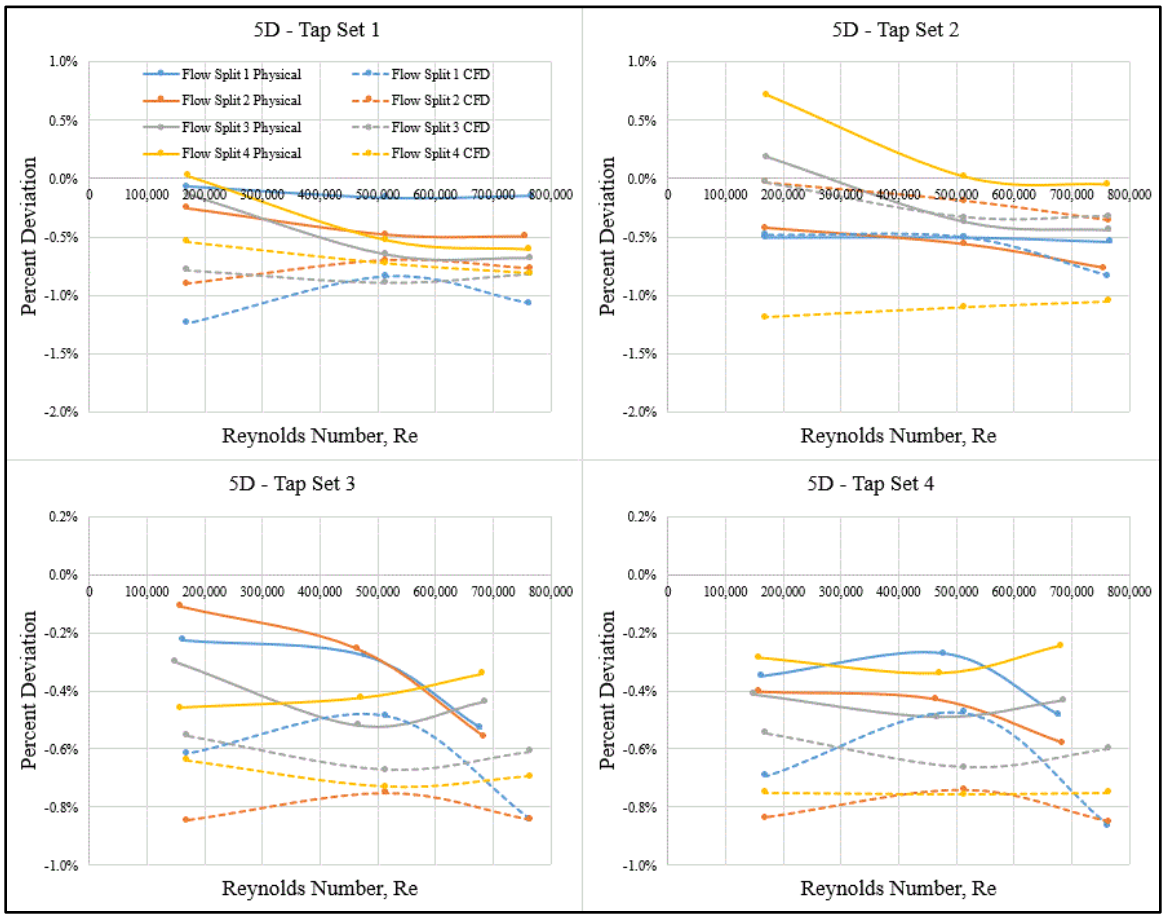

Figure 11. Physical and CFD results for all tap sets at 5D.

Figures 12 and 13 show the laboratory results with the CFD simulations for the four flow splits at 0D and 5D, respectively. From Figure 12, the overall trends are that as the flows from the north and south lines approach a 50/50 split the percent deviation between tap sets decrease. This results in a smaller variation between laboratory and CFD data at flow split three than at flow splits one, two, and four. From Figure 13, the CFD models the physical data with little deviation between taps sets. However, CFD struggles to replicate the physical trends with the exception of flow split three. The CFD results for flow split three closely follow the physical trends and yields a maximum deviation from physical data of 0.65% across all tap sets.

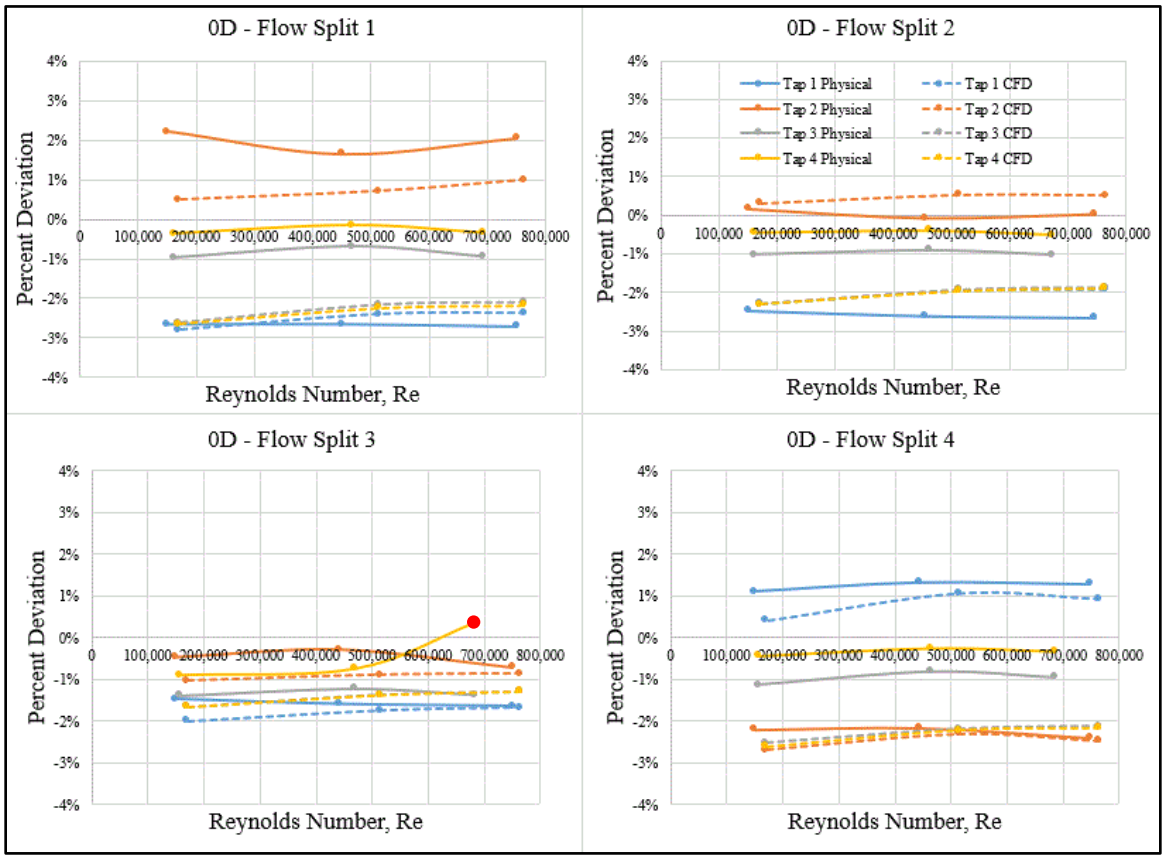

Figure 12. Physical and CFD results for all four splits at 0D

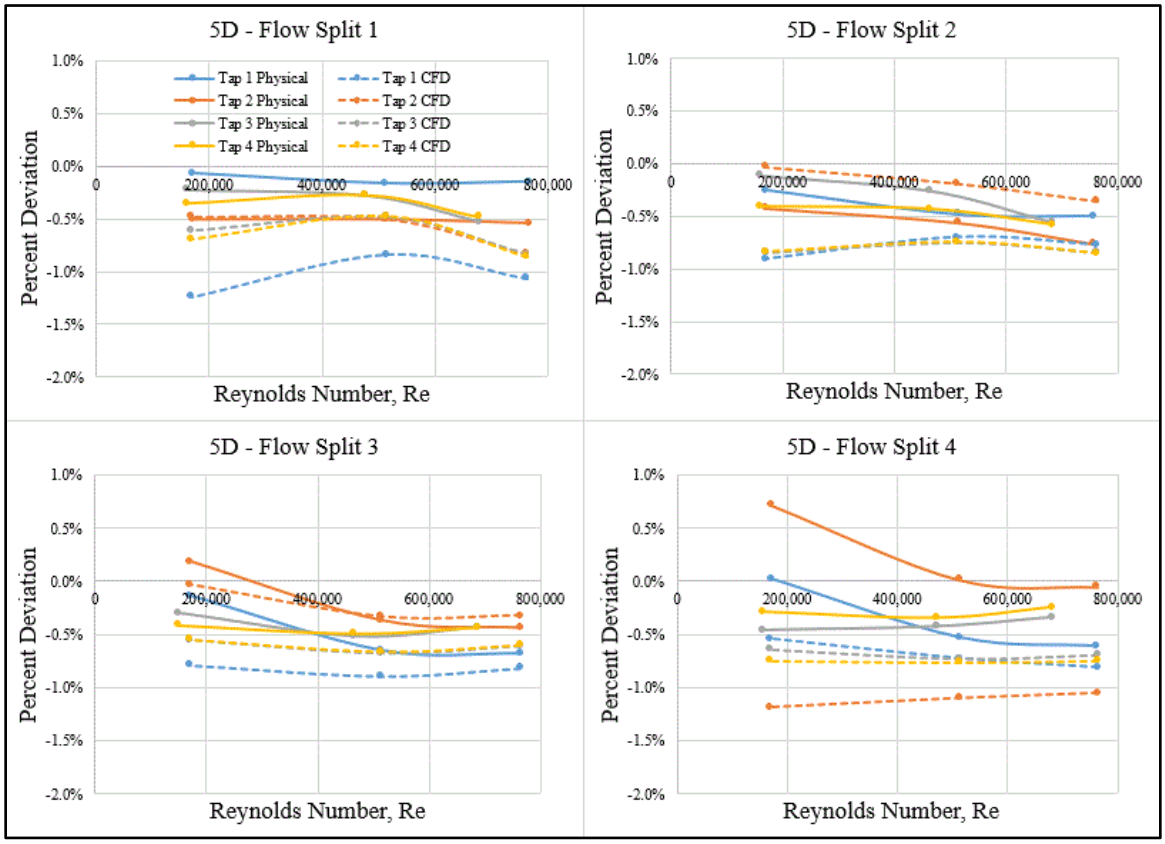

Figure 13. Physical and CFD results for all four flow splits at 5D

As expected the 0D installation was more difficult for CFD to model than the 5D installation. However, CFD still proved capable in modelling the physical trends at tap sets three and four, which allows for corrections to be made for the differences between CFD and physical data. The tap sets at 5D all performed well with the highest difference in percent deviation from physical to CFD being 1.17%, 1.90%, 0.73%, and 0.5% for tap sets one, two, three, and four respectively. Along with having the smallest differences in deviation from the physical data, tap sets three and four modelled the physical trends better than tap sets one and two at 5D as well.

Figures 14 and 15 show the flow profiles at the meter's inlet of each of the flow splits along with the straight-line test at the same Reynolds number for both 0D and 5D.

Flow split three (60/40) consistently outperforms the other flow splits because the flow profile entering the meter's inlet is comparatively more uniform. While the 50/50 flow split was not modelled in the laboratory, it can be assumed, based on the trends seen in Figures 12, 13, 14, and 15, that the 50/50 flow split would have a smaller percent deviation than the other flow splits.

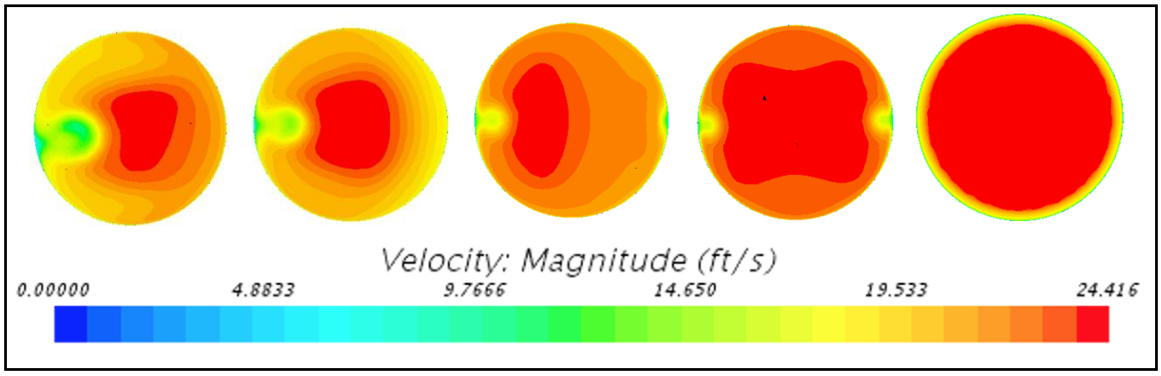

Figure 14. Flow profiles of Venturi meter's inlet for flow splits at 0D. From left to right: 100/0, 80/20, 60/40, 50/50, Straight-line

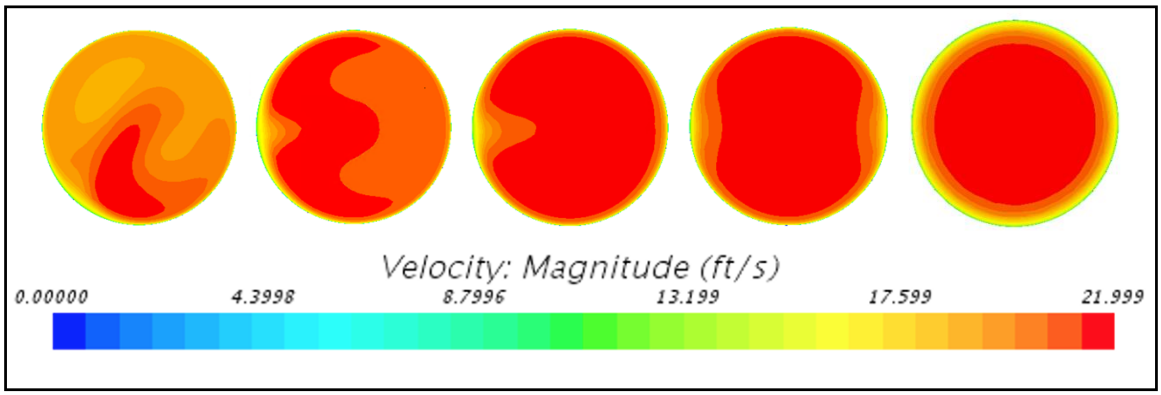

Figure 15. Flow profiles of Venturi meter's inlet for flow splits at 5D. From left to right: 100/0, 80/20, 60/40, 50/50, Straight-line

Additional CFD Models

Additional CFD models were included in this study to understand the variables that influence the CFD results. One of the additional models changed the beta ratio in the UVT from 0.7 to 0.5. Figure 16 plots the percent deviation of this model against the 0.7 beta CFD data. The 0.5 beta UVT had an overall lower percent deviation from the straight-line calibration than the 0.7 beta UVT at 5D. The author concluded that the larger beta ratio is more susceptible to the upstream disturbance because the larger throat area allowed for more pressure variation in the flow profile and therefore yielded a larger deviation.

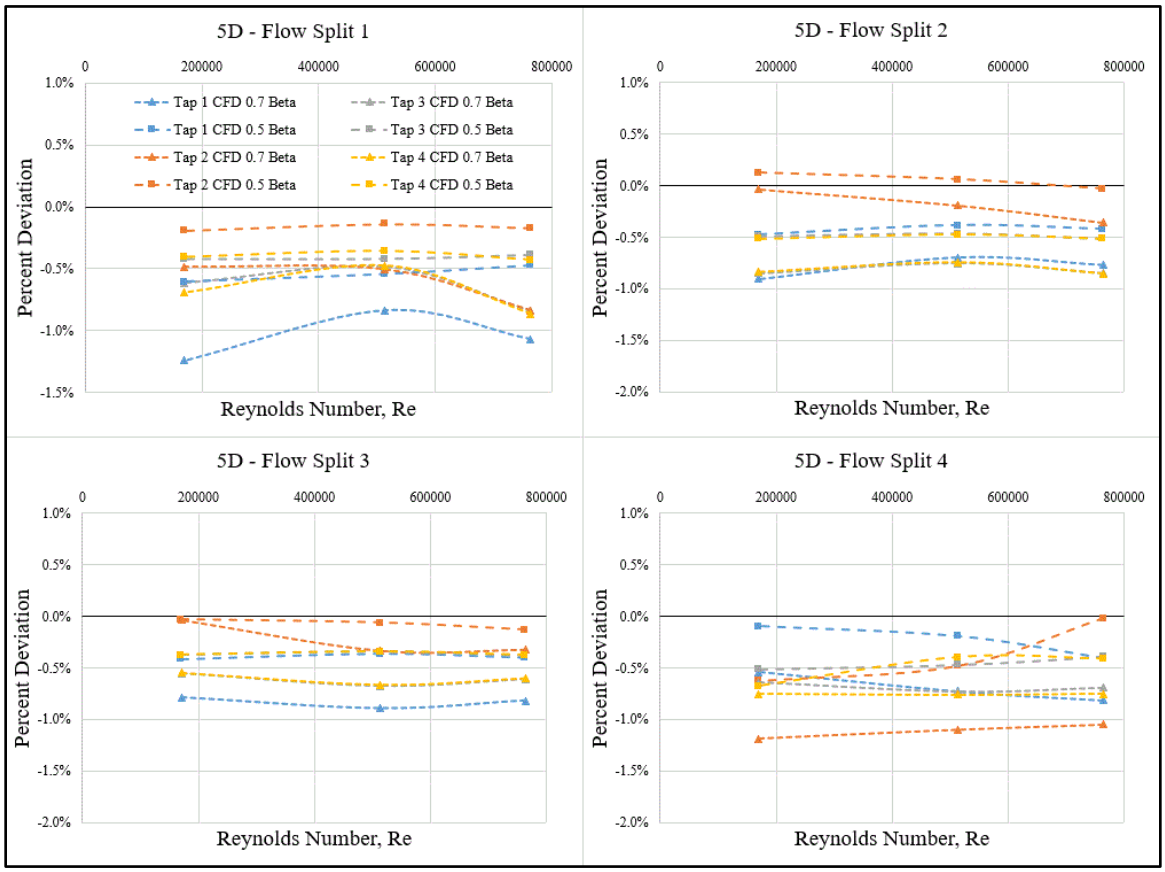

Figure 16. CFD flow split results of 0.5 and 0.7 beta UVT at 5D

The other additional model changed the geometry of the tee junction from a round-cornered tee to a sharp-cornered tee. Figure 17 plots the percent deviation of this model against the round-cornered tee CFD data. The overall trend for flow splits one, two, and four is the sharp-cornered CFD results have a higher percent deviation and are more linear with few exceptions. Flow split three shows little difference between the round-cornered and sharp-cornered tee, with the exception that the round-cornered tee approaches zero at the lower Reynolds number while the sharp-cornered tee slightly diverged.

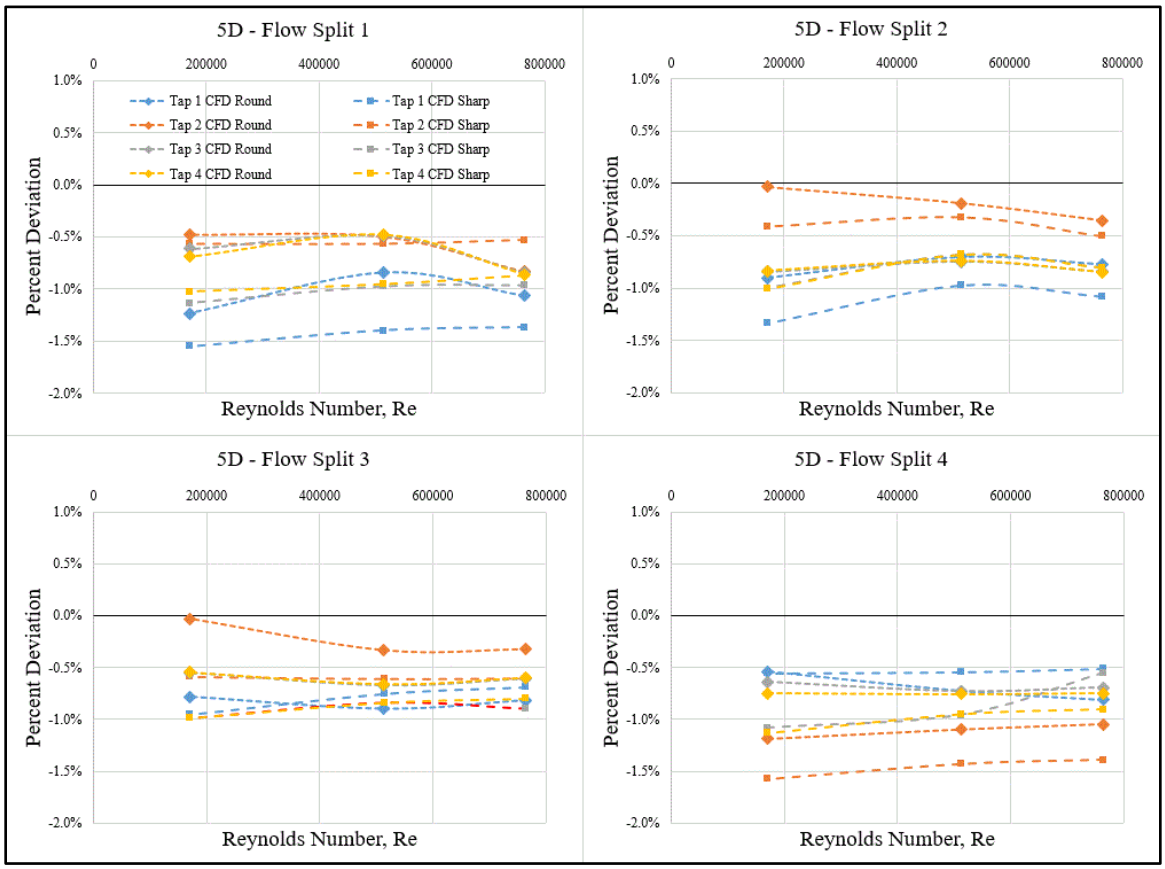

Figure 17. CFD flow split results for round-cornered and sharp-cornered tee at 5D

In addition to the sharp-cornered tee and 0.5 beta simulations, a series of 6-inch, 24-inch, and 48-inch simulations were also conducted to understand how pipe size influences the CFD results. The 6-, 24-, and 48-inch classical Venturi geometries followed the ASME PTC 19.5-2004 standard with a beta ratio of 0.5 and a converging cone half angle of 10.5 degrees and a diverging cone half angle of 7.5 degrees (ASME, 2004). Figure 18 shows the CFD data for the 6-inch, 24-inch, and 48-inch simulations plotted against percent deviation and the Reynolds number. A range of Reynolds numbers were chosen to illustrate how pipe size influences the CFD results. From the figure, its quickly apparent that the differences in the results between the three pipe diameters is insignificant, therefore, the author concluded no size effects exist.

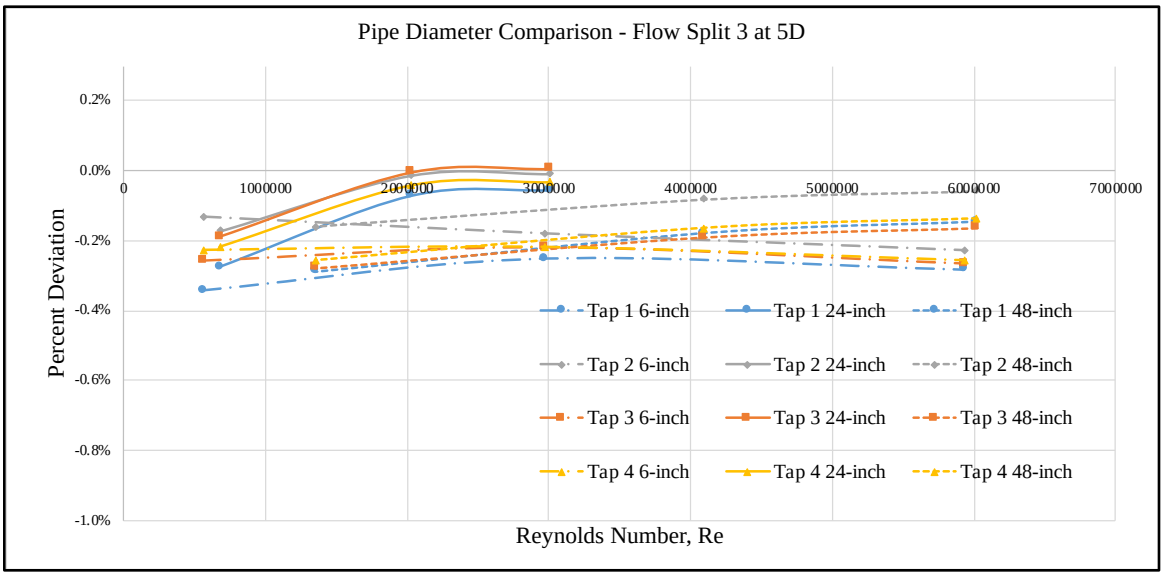

Figure 18. Flow split 3 at 5D CFD results for 6-inch, 24-inch, and 48-inch

Uncertainty of Results

The uncertainty of the physical data was calculated using the test uncertainty standard ASME PTC 19.1 2005 in which all physical results yielded an uncertainty of 0.20% or less with 95% confidence (ASME, 2006). The uncertainty in the numerical results were determined by following a procedure published by the ASME Journal of Fluids Engineering (Celik et al., 2008). The study states that three meshes be used with cell sizes that are at least 1.3 times greater than the following mesh. Using this procedure, a Grid Convergence Index (GCI) was determined for a 6-inch UVT, 24-inch classical Venturi, and a 48-inch classical Venturi, for which the GCI for discretization error did not exceed 0.05% (Table 2).

Table 2. GCI for three numerical runs

Grid Convergence Index Runs			
Parameter	6-inch	24-inch	48-inch
R_{21}	1.40	1.43	1.43
R_{32}	1.44	1.50	1.50
R_{43}			
$\phi 1$	0.9585	0.9888	0.9878
$\phi 2$	0.9579	0.9908	0.9900
$\phi 3$	0.9546	0.9907	0.9904
$\phi 4$			
P	4.7	9.1	5.3
Q(p)	-0.18	-0.43	-0.30
S	1	-1	1
ϕ^{21}_{ext}	1	1	1
ϕ^{32}_{ext}			
e^{21}_{a}	0.059%	0.198%	0.226%
e^{21}_{ext}	0.015%	0.008%	0.041%
GCI^{21}_{fine}	0.02%	0.01%	0.05%

Using the Results

This study produced laboratory and CFD discharge coefficients for a 6-inch 0.7 beta ratio UVT meter for a straight-line test and a series of tee tests. Using the discharge coefficients from tap set three at 0D, a contour plot was created for the purpose of providing an example of how this research can be used to improve the accuracy of flow measurement (Figure 19).

Example problem: A 6-inch UVT meter, with a 0.7 beta ratio, is installed close coupled (0D) to the branch of a tee junction with converging run flow. The UVT meter is rotated out of plane and has a given straight-line discharge coefficient of 0.9850. It is known that one of the converging flows has a Reynolds number of 2.5 x 10^5, a fluid density of ρ_f = 62.42 lb/ft^3, and a kinematic viscosity of ν = 1.931 x 10^{-5} ft^2/s. With the meter rotated out of plane, tap set three (top of pipe) produces a differential pressure of ΔP = 10.2 psi. It is desired to have the known converging flow to be 30% of the total flow. To solve for the actual flow split, the 30% desired flow split will be used as a guess to begin the iterative process.

Solution: First, calculate the Venturi Reynolds number (total flow).

$$Re_{meter} = \frac{Re_{branch}}{30\%} = \frac{2.5 * 10^5}{0.30} = 0.83 * 10^6$$

Using the flow split and calculated Reynolds number, a correction coefficient ($C/C_{straight}$) can be derived from Figure 17. With a flow split of 0.3 and a Reynolds number of 0.83 x 10^6, the $C/C_{straight}$ is roughly 0.9840.

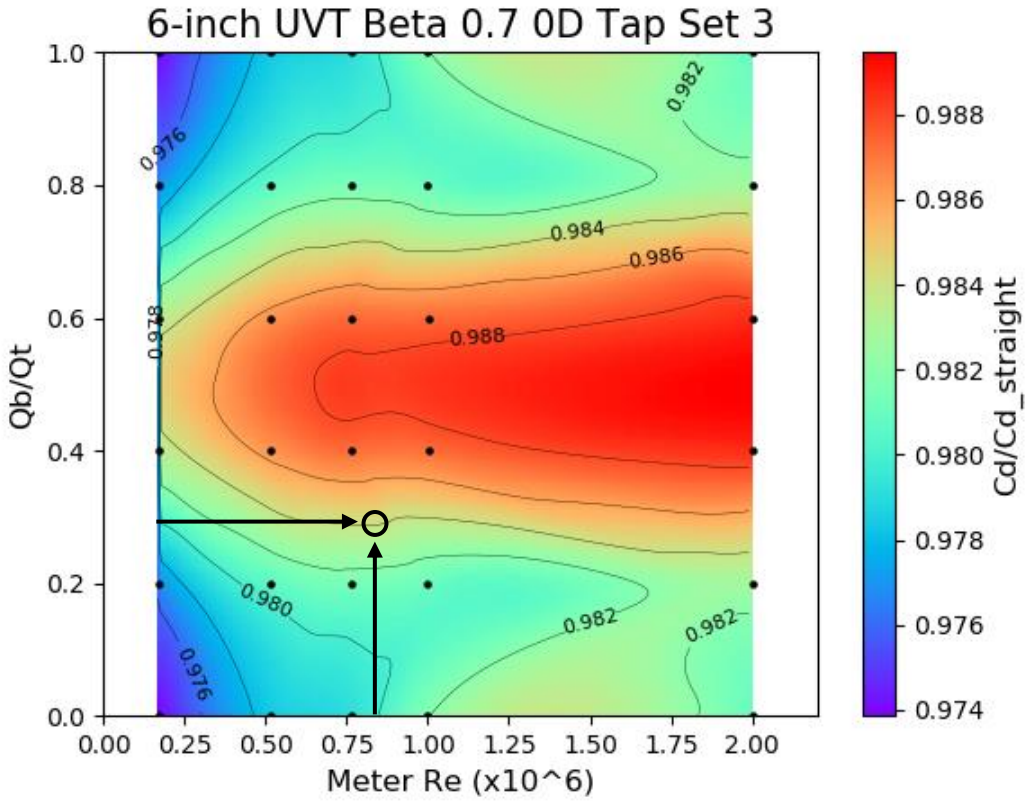

Figure 19. Contour plot for tap set three of the 6-inch 0.7 beta UVT at 0D.

The given discharge coefficient can then be adjusted using the correction coefficient.

$$\frac{C}{C_{straight}} * C_{straight}(given) = 0.9840 * 0.9850 = 0.9692$$

Convert the differential pressure from psi to psf.

$$\Delta P = 10.2 \frac{lb}{in^2} * 144 \frac{in^2}{ft^2} = 1468.80 \frac{lb}{ft^2}$$

Calculate the area of the throat section of the UVT.

$$A_t = \frac{\pi}{4} * \left(\frac{6 * 0.7}{12}\right)^2 = 0.0962\ ft^2$$

Calculate the flow rate, Q, using the Venturi equation (equation 1).

$$Q = 0.9692 * 0.0962 * \sqrt{\frac{2 * 32.2 * 1468.80}{(1 - 0.7^4) * 62.42}} = 4.16 \frac{ft^3}{s}$$

Calculate the adjusted Reynolds number using the flow rate just found.

$$Re_{meter} = \frac{VD}{\nu} = \frac{4.16 * \left(\frac{6}{12}\right)}{\left(\frac{\pi}{4} * \left(\frac{6}{12}\right)^2\right) * 1.931 * 10^{-5}} = 0.55 * 10^6$$

Calculate the new flow split using the meter Reynolds number just calculated and the known branch Reynolds number.

$$Flow\ split = \frac{0.25 * 10^6}{0.55 * 10^6} * 100 = 45.52\%$$

The solution process now becomes iterative by finding a new correction coefficient using the calculated flow split and meter Reynolds number. Within three iterations the solution converged to a flow split of 45.38% with the last iteration changing the flow split by just 0.01%. With the desired flow split being 30%, the process would be repeated after having adjusted the control valves. For this example, the solution was considered converged once the solution changed by 0.02% or less.

If the flow rate were to be calculated for this example with the given *C* (0.9850) the flow rate would be 4.23 cfs. The percent difference between the flow rates of the adjusted discharge coefficient and the straight-line discharge coefficient is 1.3%. The percent difference provides insight into the importance of flow calibration and why a straight-line discharge coefficient is not suitable for an installation with disturbed flow conditions. As the flow split approaches a ratio of 100/0, it is expected that the percent difference would increase. Likewise, it is expected the percent difference would increase as the total flow decreases.

CHAPTER VI

CONCLUSIONS

Venturi meters are one of the most widely used flow measurement devices throughout the world. To ensure accurate flow measurement is achieved, a substantial amount of research has been geared towards determining the required pipe diameters needed between pipe fittings and the Venturi meter. Yet none had previously researched how a tee junction with converging flow through the run would affect a Venturi meter installed on the branch.

Both physical and numerical modelling were used in this research. The physical testing consisted of a straight-line test and a series of tee tests using a 6-inch, 0.7 beta, UVT meter. The numerical testing was conducted using Star-CCM+ and consisted of testing different Venturi meter geometries, tee geometries, beta ratios, and pipe sizes. The results of this study were plotted as graphs of percent deviation versus meter Reynolds number and contour plots of discharge coefficient ratios plotted against flow split and meter Reynolds number.

While CFD capably modelled the 0D and 5D installations across all tap sets and flow splits, flow split three and tap set three best simulated the physical trends with the smallest variation from physical data. It should be noted that the graphs and contour plots provided in this thesis are specific to a 6-inch UVT at a Reynolds number that didn't exceed 1 million. Further research could investigate the impact of higher Reynolds numbers, compressible fluids, or different Venturi geometries.

A summary of key findings is as follows:

1. CFD is capable of modelling laboratory trends of discharge coefficients of a Venturi meter installed on the branch of a tee junction with converging run flow.
2. Correction factors for the provided straight-line discharge coefficient can be developed across a range of flow splits and Reynolds numbers from physical or CFD results.
3. As the flow split in the run converges towards a 50/50 split, the percent difference between CFD and physical data decreases.
4. The Venturi meter installed out of plane (tap sets three and four) consistently produced a predictable difference between CFD and physical data across all flow splits.
5. Flow split one for tap set one and flow split four for tap set two proved to be difficult configurations for CFD to model. These configurations should be avoided.
6. The 0.7 beta ratio was found to deviate from the straight-line calibration more than the 0.5 beta ratio.
7. The sharp-cornered tee on average shifted the trend lines down resulting in a higher percent deviation from the straight-line calibration.
8. Pipe size has little effect on the CFD results.

REFERENCES

Abdulwahhab, M., Injeti, N.K., Dakhil, S.F., *Numerical Prediction of Pressure Loss of Fluid in a T-Junction.* 2013. Journal of Energy and Environment. Vol. 4, No. 2.

Celik, I.B., Ghia, U., Roache, P.J., Freitas, C.J., Coleman, H., and Raad, P.E. (2008). *Procedure for Estimation and Reporting of Uncertainty Due to Discretization in CFD Applications.* Journal of Fluids Engineering-Transactions of the ASME, 130, 078001-3.

Costa, N.P., Maia, R., Proenca, M. F. and Pinho, F. T. 2006. *Edge Effects on the Flow Characteristics in a 90 deg Tee Junction*. November 2006. ASME. *J. Fluids Eng*. 128(6): 1204-1217

Finnemore, E.J. and Franzini, J.B., *Fluid Mechanics with Engineering Applications*. 2006. 10th Ed., McGraw-Hill, New York. pp. 515

Sandberg, Benjamin G., *Venturi Flowmeter Performance Installed Downstream of the Branch of a Tee Junction*. 2020. *All Graduate Theses and Dissertations*. 7825.

Sharp, Z.B., Johnson, M.C., Barfuss, S.L., and Rahmeyer, W.J. 2009. *Energy Losses in Cross Junctions.* Journal of Hydraulic Engineering, Vol. 136, No. 1, January 2010.

Stauffer, T., Johnson, M.C., Barfuss, S.L., and Sorensen, A.D., *Hydraulic Average of Multiple Tap Sets to Improve Performance of Venturi Flowmeters with Upstream Disturbance*. 2019. *All Graduate Theses and Dissertations*. 7487.

The American Society of Mechanical Engineers (ASME), comp. *Addeneda to ASME MFC-3M-2004: Measurement of Fluid Flow in Pipes Using Orifice, Nozzle, and Venturi.* March 24, 2008. ASME code, Three Park Avenue, New York. pp.75

The American Society of Mechanical Engineers (ASME), *Test uncertainty: An American national standard*. 2006. ASME PTC 19.1- 2005, New York.

The American Society of Mechanical Engineers (ASME), *Flow Measurement, Performance Test Codes.* 2004. ASME PTC 19.5-2004, New York. pp. 49-52

APPENDICES

APPENDIX A: Laboratory Testing Figures

Figure A1. 0D laboratory testing of tap sets 1 and 2.

Figure A2. 0D laboratory testing of tap sets 3 and 4

Figure A3. 5D laboratory testing of tap sets 1 and 2

Figure A4. Instrumentation used for flow and differential pressure measurement

APPENDIX B: Contour Plots

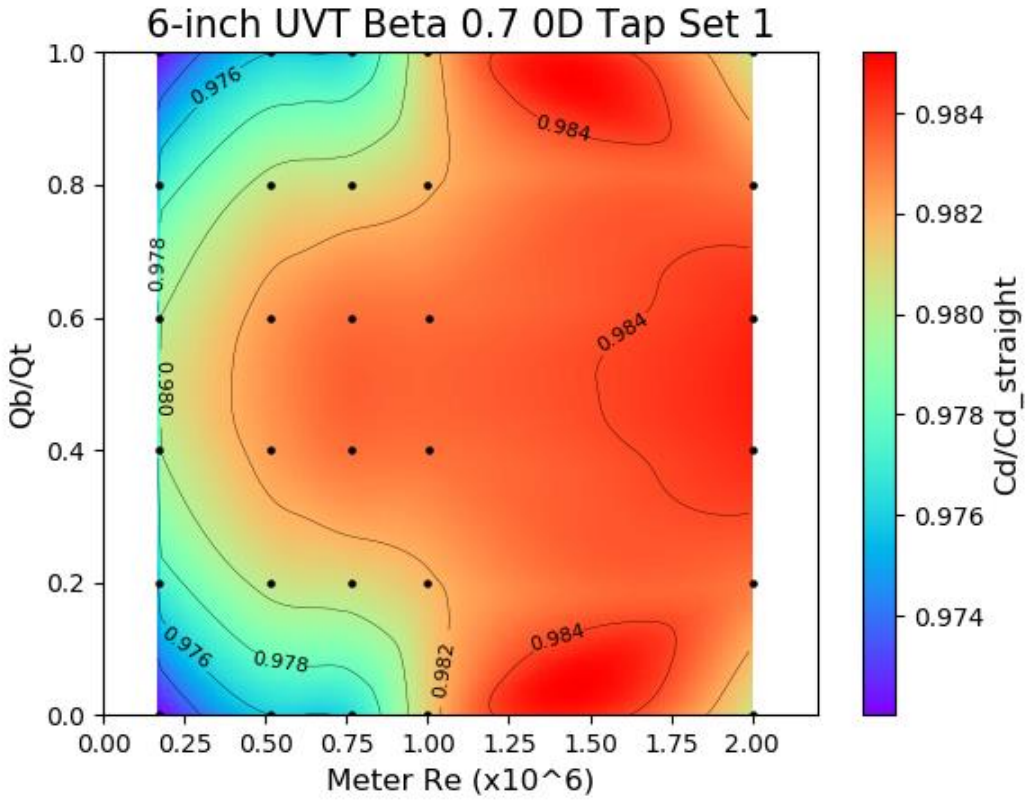

Figure B1. Contour plot for tap set 1 of the CFD 6-inch 0.7 beta UVT at 0D

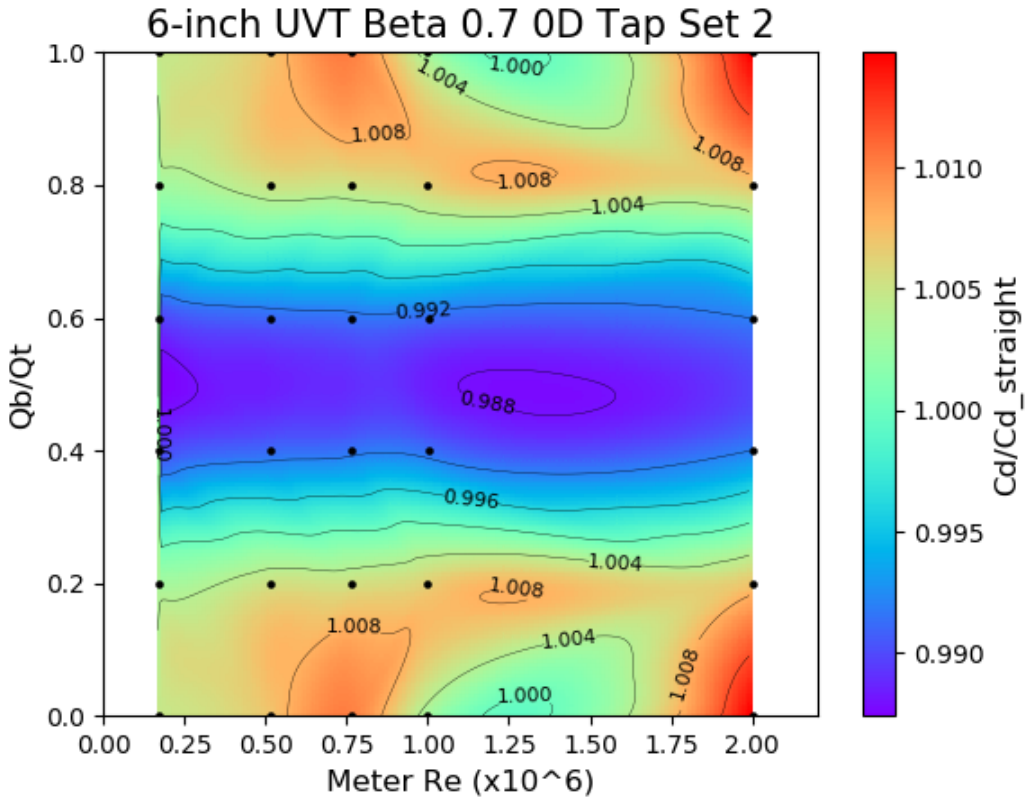

Figure B2. Contour plot for tap set 2 of the CFD 6-inch 0.7 beta UVT at 0D

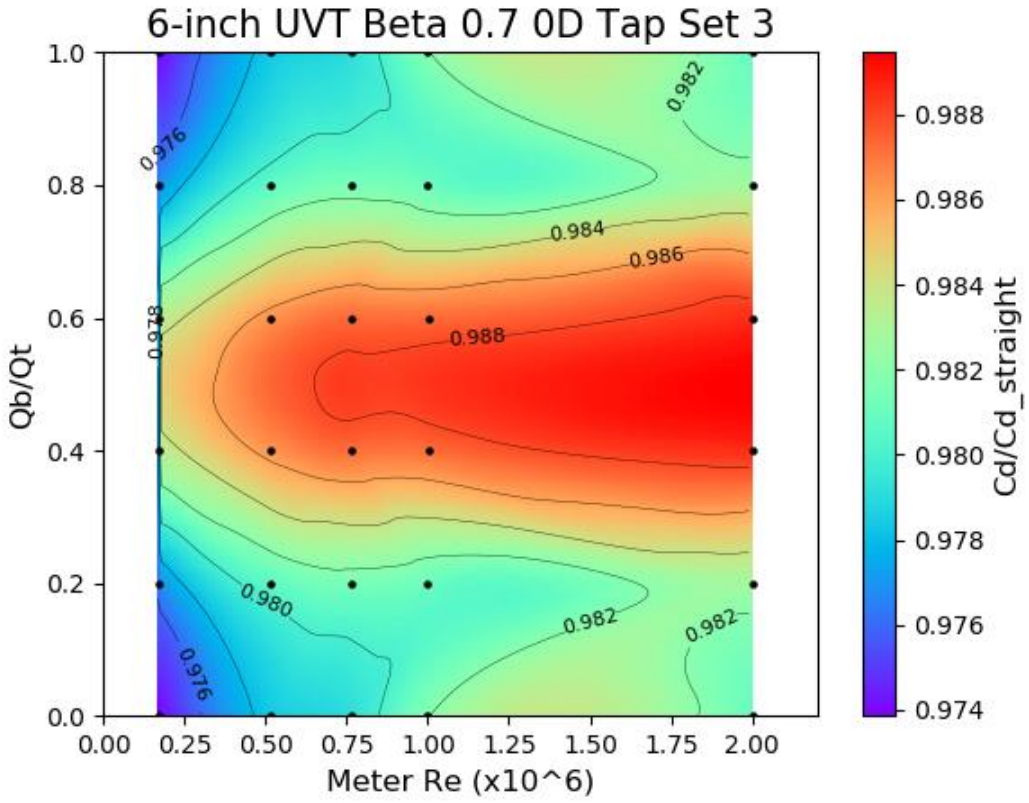

Figure B3. Contour plot for tap set 3 of the CFD 6-inch 0.7 beta UVT at 0D

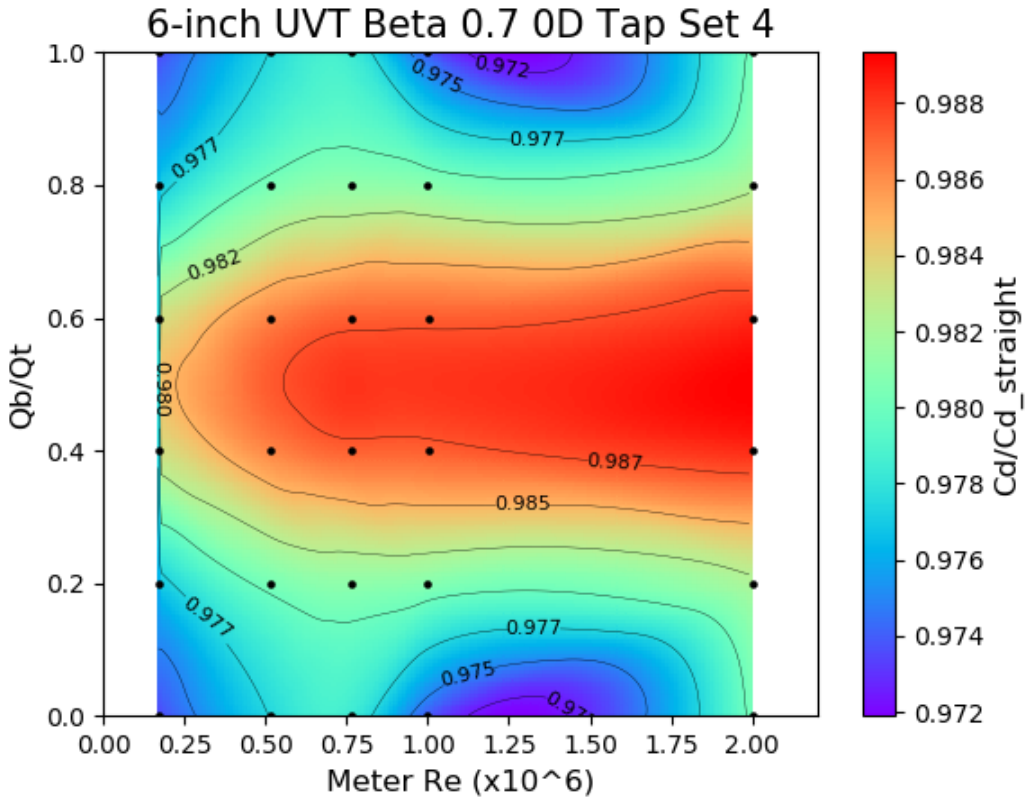

Figure B4. Contour plot for tap set 4 of the CFD 6-inch 0.7 beta UVT at 0D

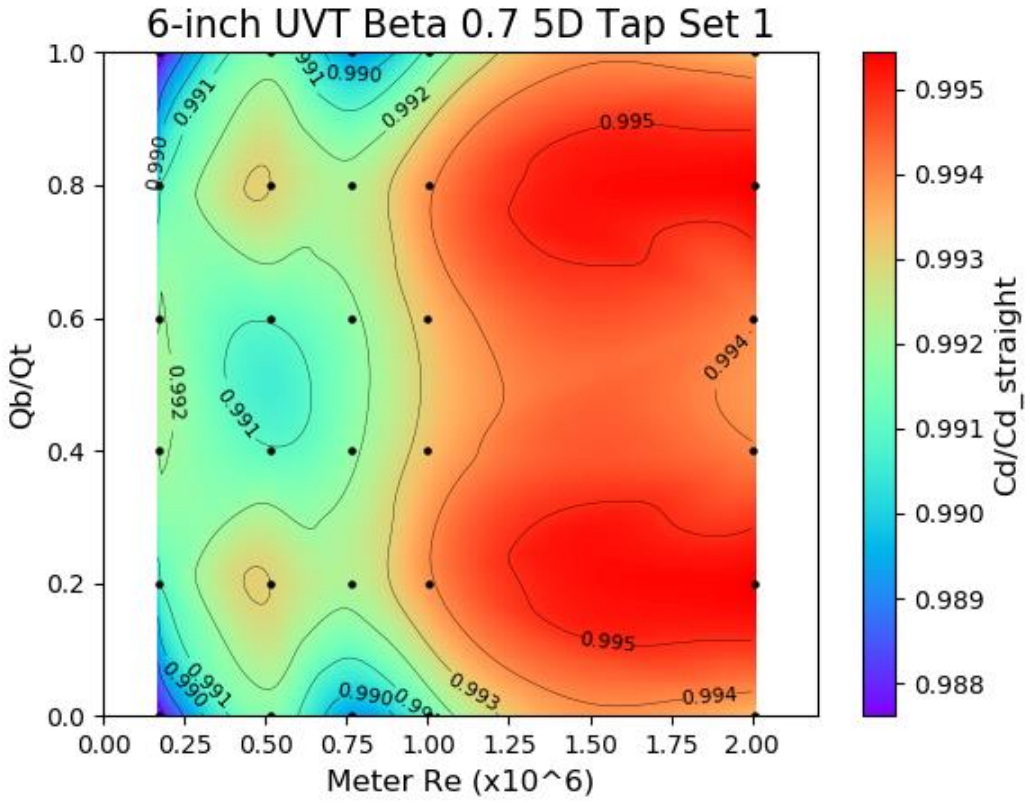

Figure B5. Contour plot for tap set 1 of the CFD 6-inch 0.7 beta UVT at 5D

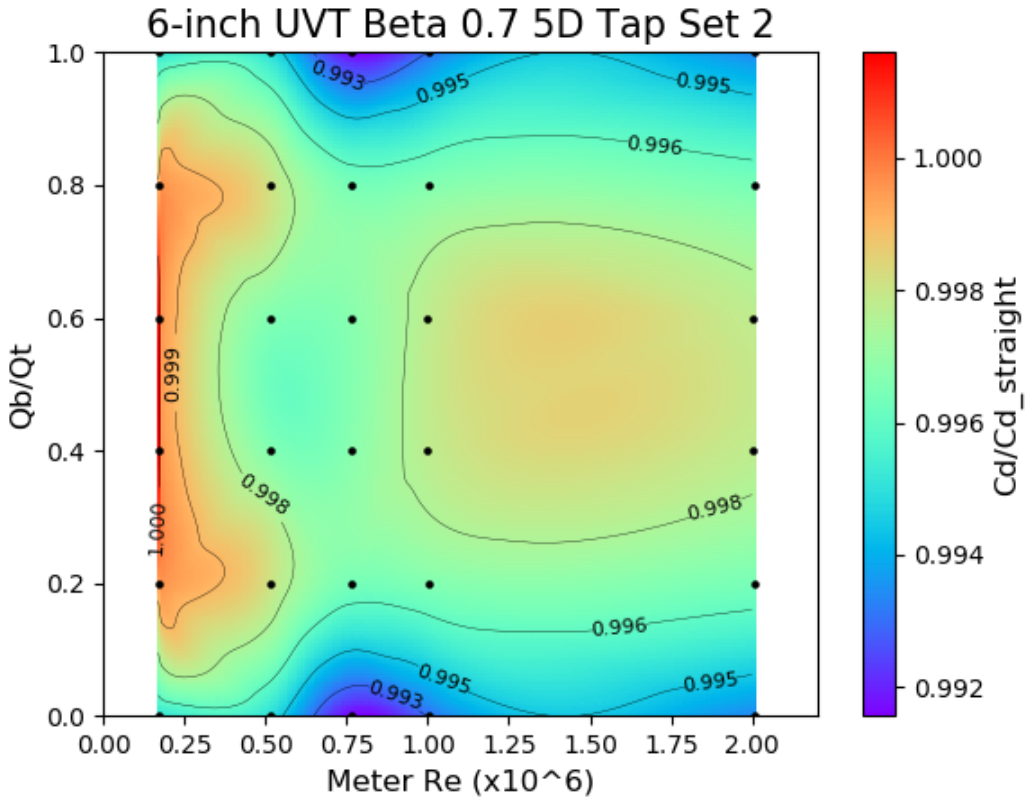

Figure B6. Contour plot for tap set 2 of the CFD 6-inch 0.7 beta UVT at 5D

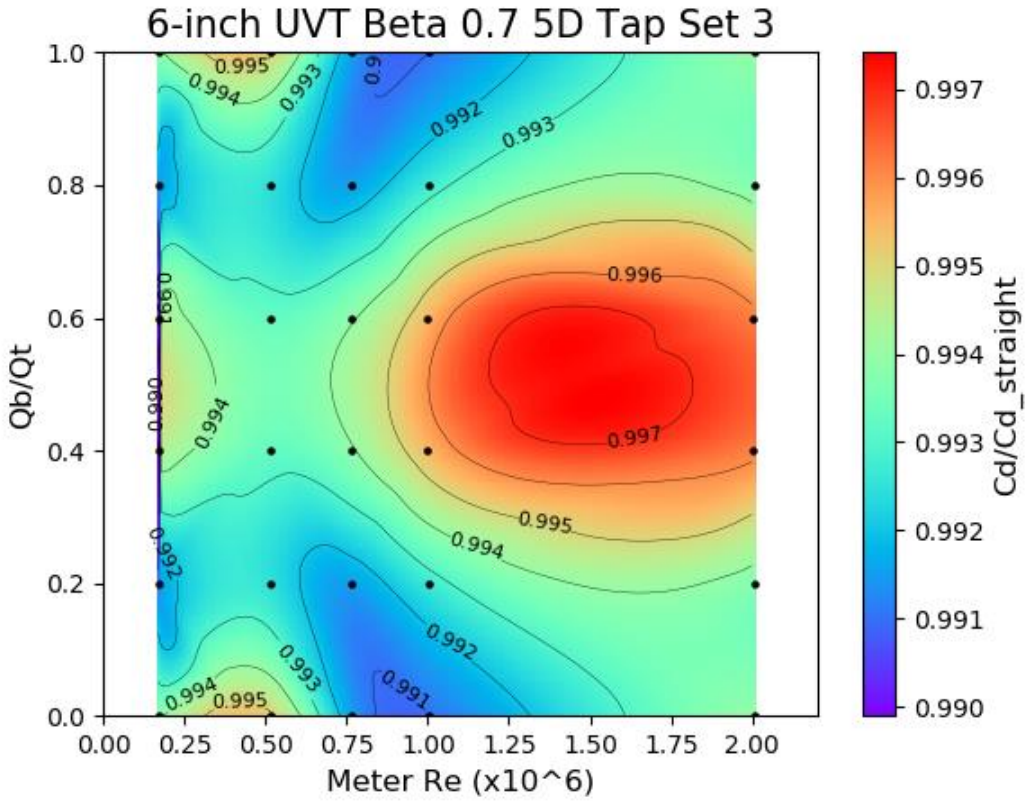

Figure B7. Contour plot for tap set 3 of the CFD 6-inch 0.7 beta UVT at 5D

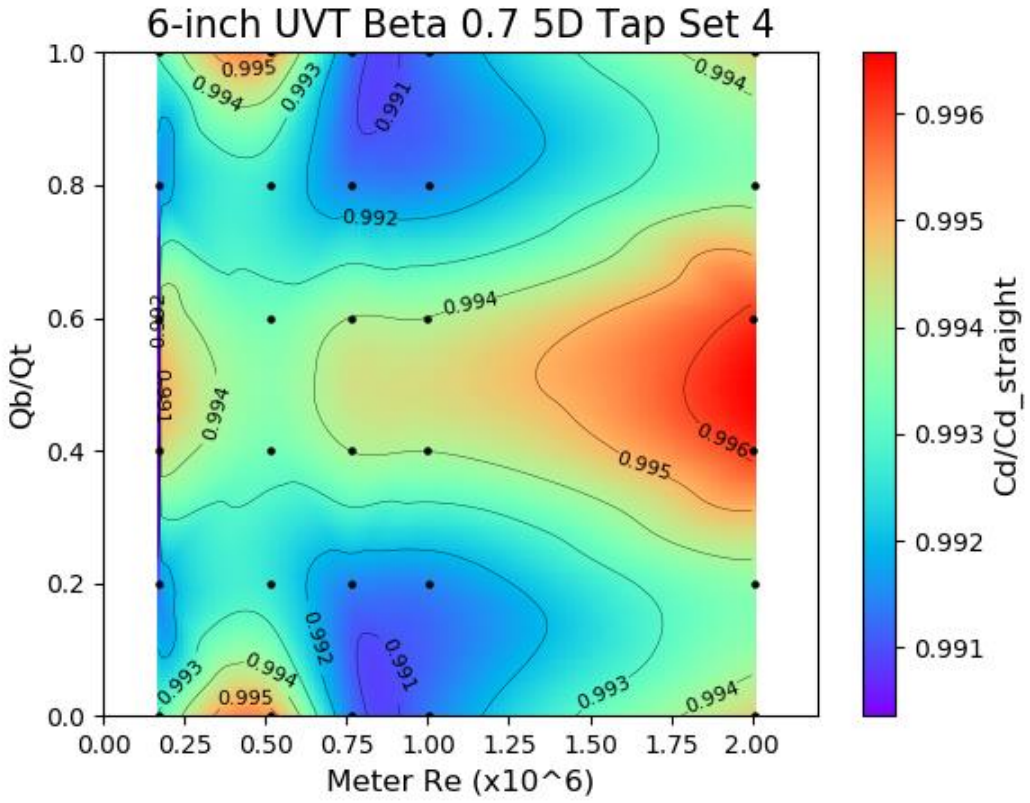

Figure B8. Contour plot for tap set 4 of the CFD 6-inch 0.7 beta UVT at 5D

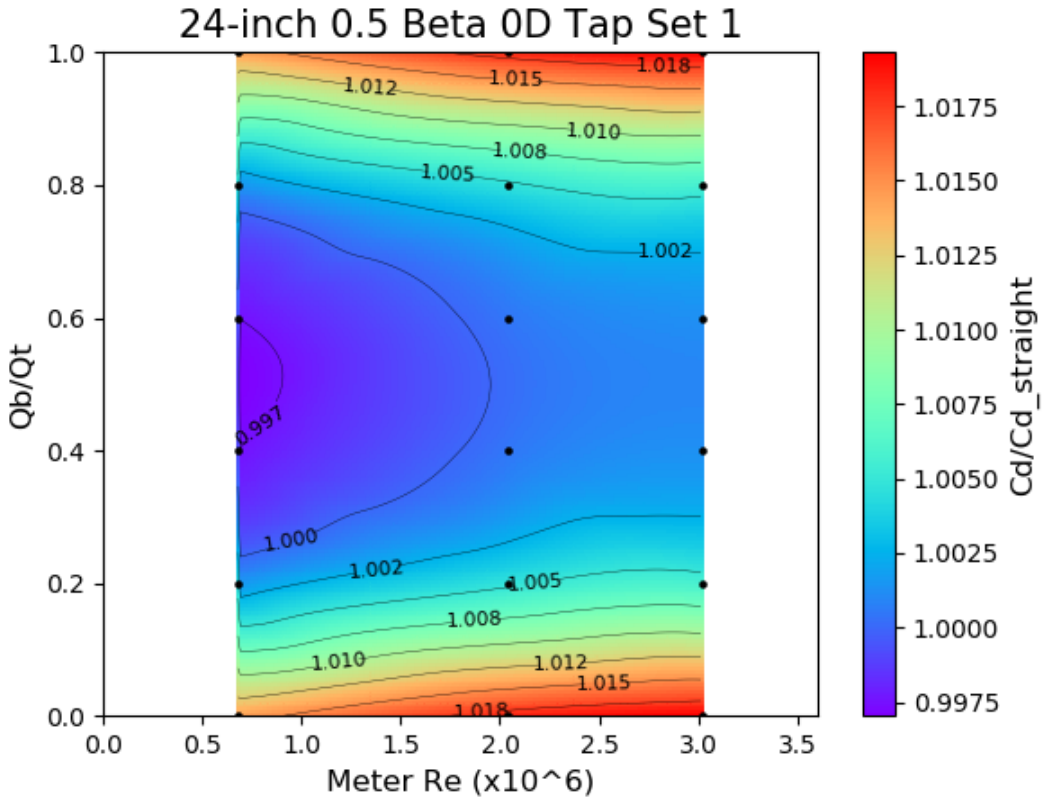

Figure B9. Contour plot for tap set 1 of the CFD 24-inch 0.5 beta classical Venturi meter at 0D

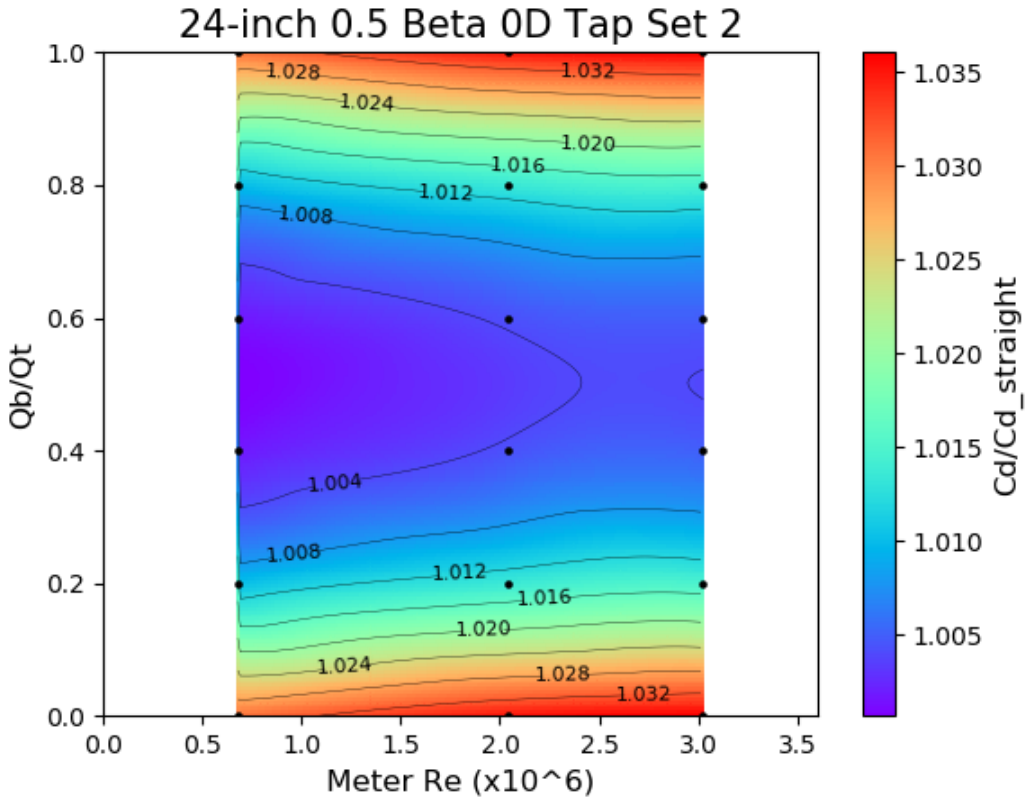

Figure B10. Contour plot for tap set 2 of the CFD 24-inch 0.5 beta classical Venturi meter at 0D

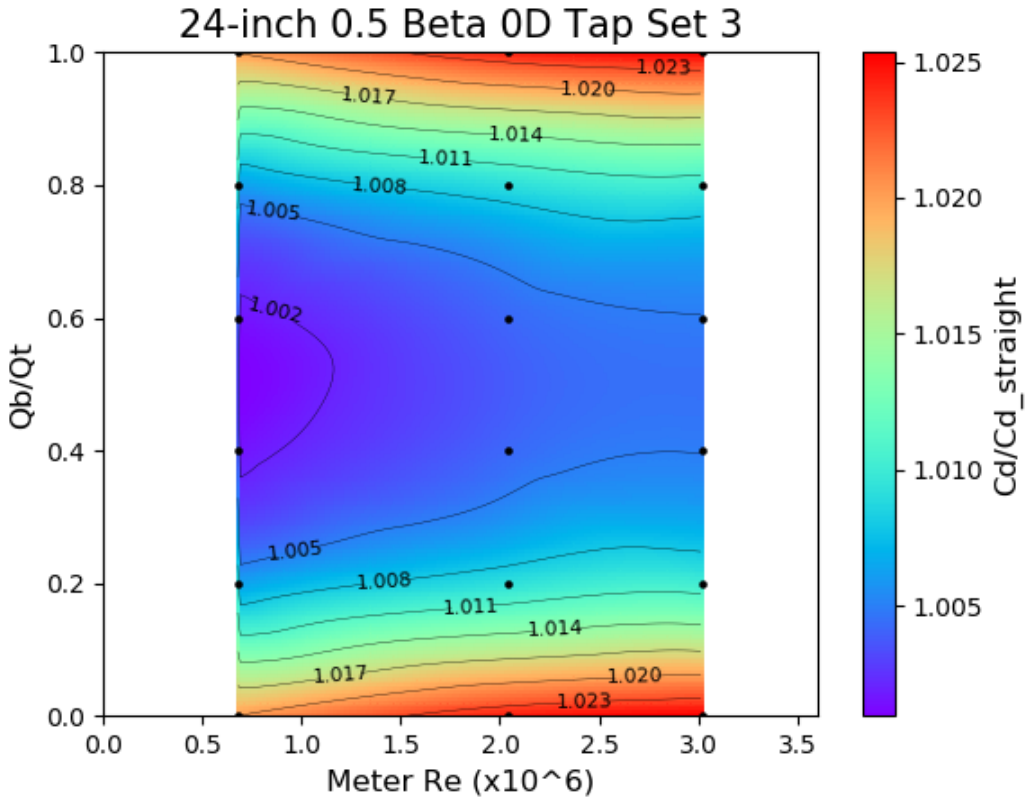

Figure B11. Contour plot for tap set 3 of the CFD 24-inch 0.5 beta classical Venturi meter at 0D

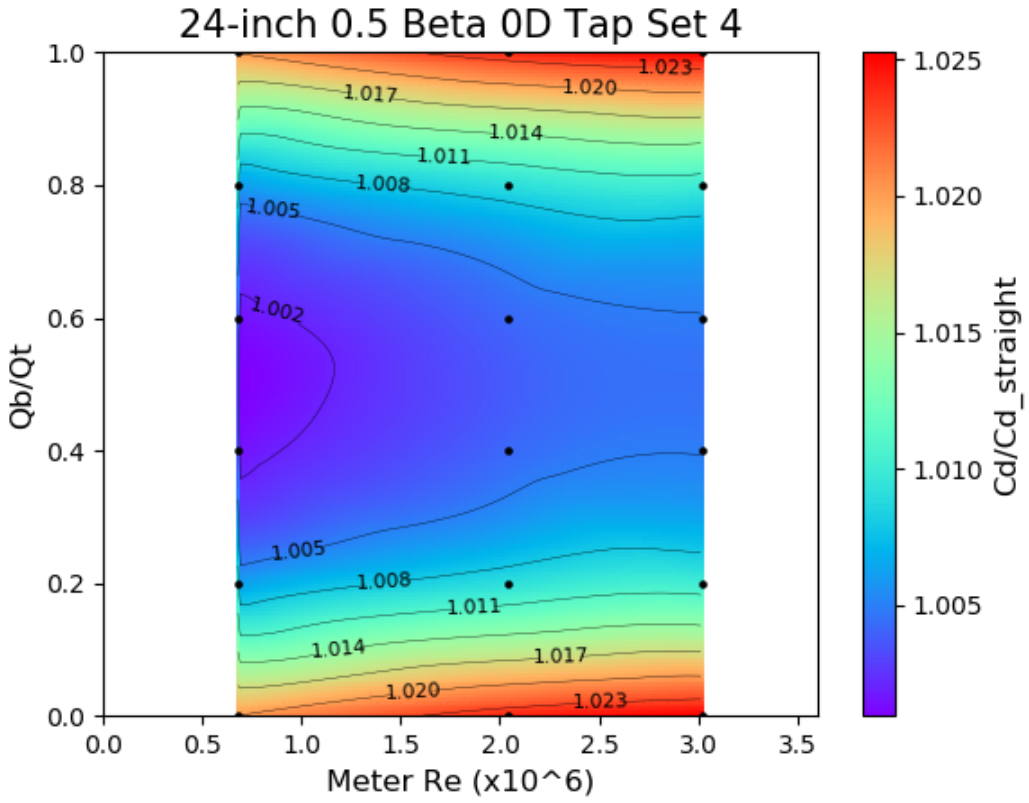

Figure B12. Contour plot for tap set 4 of the CFD 24-inch 0.5 beta classical Venturi meter at 0D

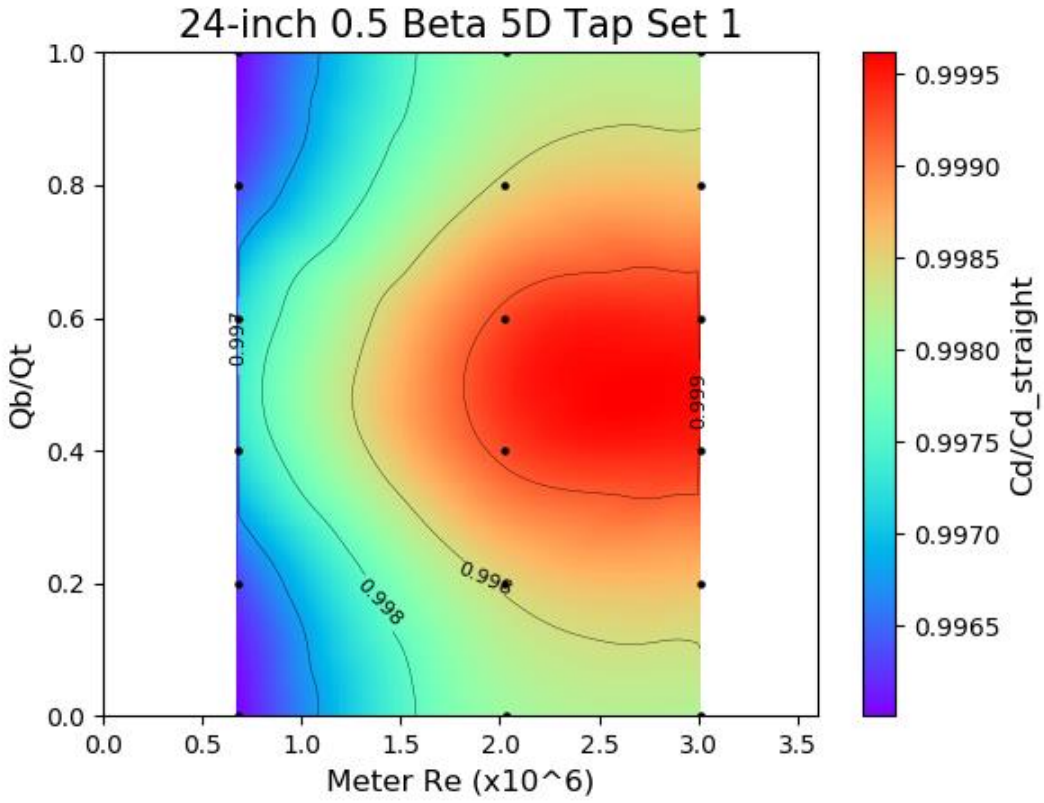

Figure B13. Contour plot for tap set 1 of the CFD 24-inch 0.5 beta classical Venturi meter at 5D

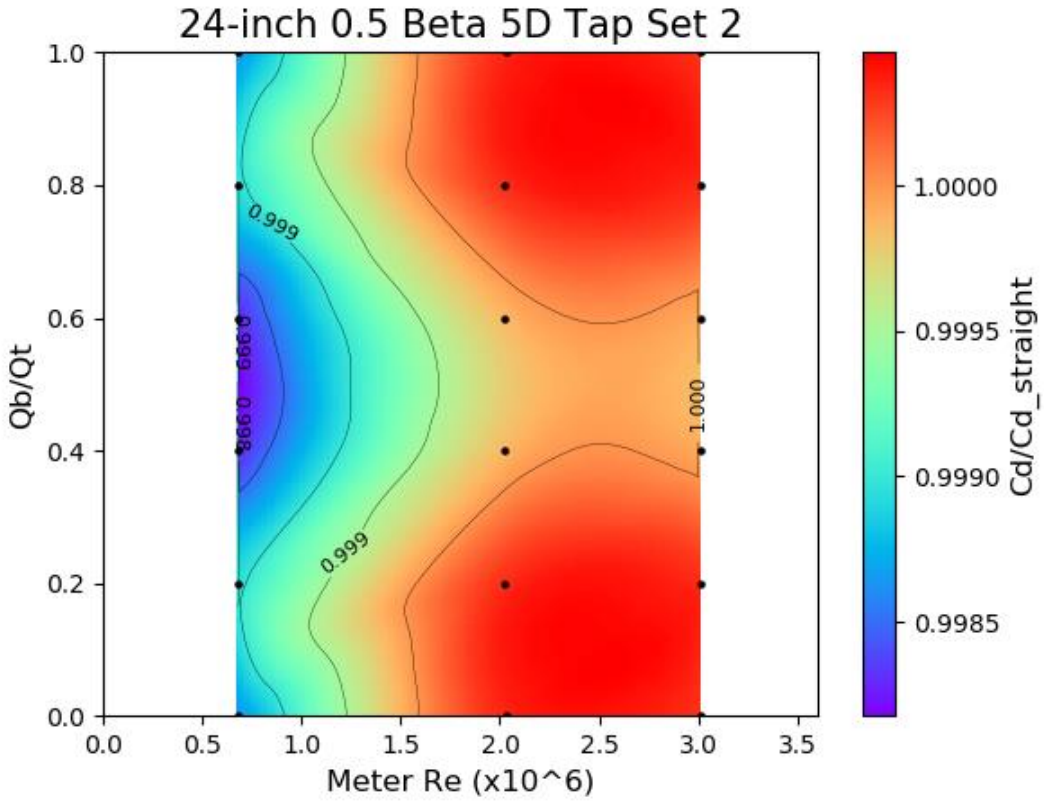

Figure B14. Contour plot for tap set 2 of the CFD 24-inch 0.5 beta classical Venturi meter at 5D

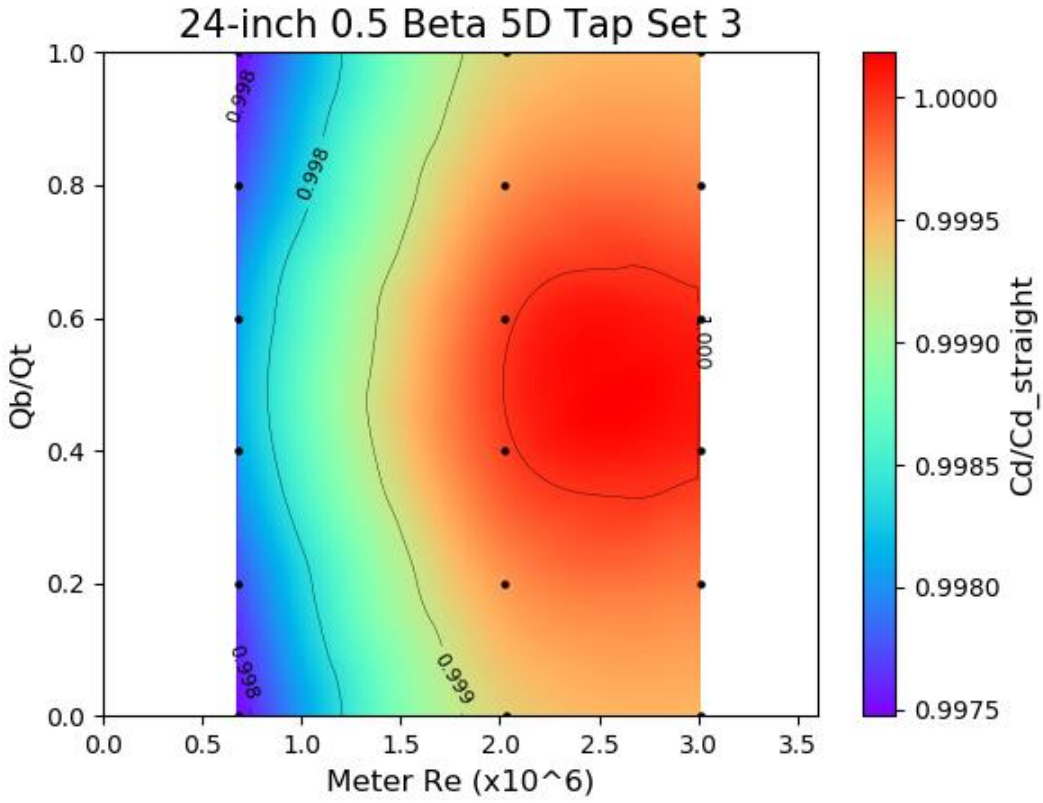

Figure B15. Contour plot for tap set 3 of the CFD 24-inch 0.5 beta classical Venturi meter at 5D

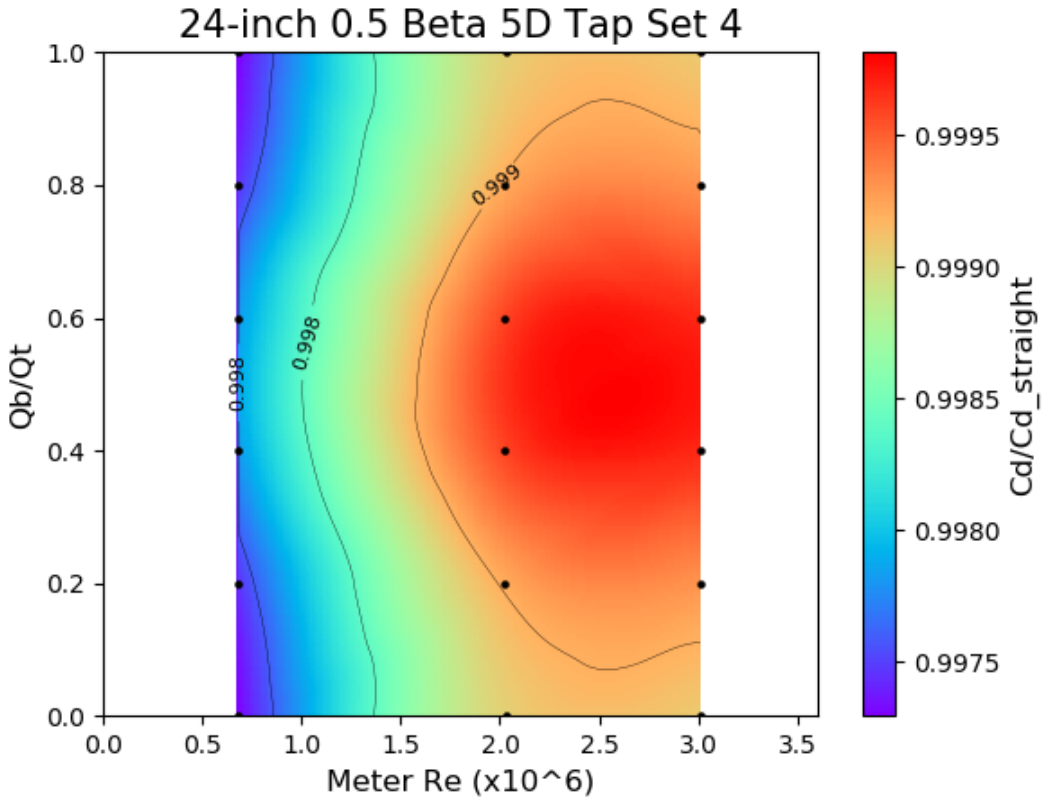

Figure B16. Contour plot for tap set 4 of the CFD 24-inch 0.5 beta classical Venturi meter at 5D